의학박사 학위논문

The role of glutaminase 1 in the development of airway hyperresponsiveness in high-fat diet-fed mice

고지방식이 마우스의 기도과민성 발생에서 글루타민분해효소의 역할

2022년 8월

서울대학교 대학원

의과대학 의학과 내과학

심 지 수

고지방식이 마우스의 기도과민성 발생에서 글루타민분해효소의 역할

지도 교수 박 홍 우

이 논문을 의학박사 학위논문으로 제출함
2022년 4월

서울대학교 대학원
의학과 내과학 전공
심 지 수

심지수의 의학박사 학위논문을 인준함
2022년 7월

위 원 장 임 재 준 (인)

부위원장 박 홍 우 (인)

위 원 박 진 균 (인)

위 원 서 동 인 (인)

위 원 김 병 근 (인)

Abstract

The role of glutaminase 1 in the development of airway hyperresponsiveness in high-fat diet-fed mice

Ji-Su Shim

Department of Internal Medicine

Graduate School of Medicine

Seoul National University

Background: Airway hyperresponsiveness (AHR) is a major asthma feature and is associated with obesity, which is defined by the body mass index (BMI). However, body mass is composed of fat mass (FM) and muscle mass (MM), and compositions of FM and MM change over time. In this sense, a longitudinal study focused on FM changes over time is needed to confirm the causal relationship between obesity and AHR. Recently, it has been reported that metabolism is closely related to the immune system, particularly glutamine metabolism is known to be altered in obese patients resulting in increased inflammation. In line with this thinking, altered glutamine metabolism may link obesity with AHR. However, there is a lack of studies focused on glutamine metabolism and obesity-induced AHR.

Methods: A cross-sectional and long-term longitudinal study was performed to evaluate the causal relationship between obesity and AHR development using data from the Seoul National University Hospital Healthcare System Gangnam Center. Healthy individuals who underwent two methacholine bronchial provocation tests (MBPTs) with a follow-up period of more than three years (between the first and second tests) were enrolled in the longitudinal study. All participants showed a negative AHR at the first health checkup. Participants had a bioelectrical impedance analysis (BIA) done at every health checkup, which provided the FM index (FMI; FM is normalized for height) and MM index (MMI; MM is normalized for height). Changes in FMI and MMI of individuals who had become positive for AHR were compared with the FMI and MMI of individuals who stayed negative for AHR. Next, an animal experiment was conducted to investigate the role of glutamine metabolism in the development of obesity-induced AHR. Four-week-old male C57BL/6 mice were fed a high-fat diet (HFD) for 13 weeks in the presence or absence of Bis-2-(5-phenylacetamido-1,3,4-thiadiazol-2-yl)ethyl sulfide (BPTES), a selective inhibitor of glutaminase 1 (GLS1), which converts glutamine to glutamate. The blood, lung, and adipose tissue of mice were analyzed. Then, in vitro experiments were done using mouse bone marrow-derived macrophages (BMDMs) and alveolar macrophage cell lines. Furthermore, plasma glutamine and glutamate levels of obese and non-obese asthmatic patients were analyzed.

Results: A total of 4,023 individuals were enrolled in the cross-sectional analysis (1,290 females and 2,733 males). Among them, 112 individuals tested positive for AHR (AHR_{pos}) at the first health checkup. Multivariate analyses showed that the risk of having AHR was significantly associated with FMI values (odds ratio [OR] = 1.37,

95% confidence interval [CI]: 1.06–1.76, p = 0.017), but there was no association with MMI values. FMI values also showed a significant negative correlation with PC20 values in the AHR_{pos} group (R = -0.31, p = 0.00087), while MMI values showed no correlation with PC20 values.

Next, a total of 283 individuals (61 females and 267 males) were included in the longitudinal analysis of healthy individuals. The mean number of segmental BIA measurements was 6.96 (interquartile range (IQR): 5–9), and the mean follow-up period was 6.69 years (IQR: 4.63–8.36). Among them, 13 individuals became positive for AHR (AHR_{pos} conversion group), whereas the rest stayed persistently negative for AHR (AHR_{neg} conversion group). During the follow-up period, all individuals had gained FM and lost MM. Individuals in the AHR_{pos} conversion group gained more FM than those in the AHR_{neg} conversion group, although the statistical significance was weak (p = 0.057). A multivariate analysis showed that an increased FMI change rate ([kg/m^2]/year) was significantly associated with the risk of developing AHR (OR = 1.114x10^4, 95% CI: 1.192–1.551x10^8, p = 0.037).

BPTES treatment prevented HFD-induced AHR and significantly decreased IL-1β$^+$ classically activated macrophages (M1s) and type 3 innate lymphoid cells (ILC3s) which increased in the lungs of HFD-fed obese mice. In in vitro experiments, BPTES treatment or glutamine supplement significantly reduced the proportion of IL-1β$^+$NLRP3$^+$ M1s in lipopolysaccharide-stimulated BMDMs and mouse alveolar macrophage cell lines. BPTES treatment also significantly reduced the IL-17 producing ILC3s differentiated from ILCs in naïve mouse lung. In addition, plasma glutamate/glutamine ratios were significantly higher in obese asthmatics compared to non-obese asthmatics.

Conclusion: In this longitudinal study using the health checkup database, it was confirmed that a gain of FM over time is a risk factor for the development of AHR in healthy individuals. In the animal experiment, it was observed that altered glutamine metabolism had a role in the development of AHR induced by an HFD. IL-1β^{+}NLRP3^{+} M1s and ILC3s are key immune cells in the pathogenesis of HFD-induced AHR, which is reversed by inhibiting the first step of glutaminolysis. Following this study, there is a need for a prospective study to assess the role of FM reduction and dietary glutamine supplementation in preventing AHR development in obese individuals.

Keywords:

Asthma; airway hyperresponsiveness; fat mass; obesity; glutamine; high-fat diet-fed mice; innate lymphoid cells; macrophages.

Student Number:

2017-33616

Table of Contents

Introduction

Obesity is one of the important risk factors and disease modifiers for asthma (1). Several epidemiologic studies suggested an association between obesity and asthma in adults (2-5). It has been reported that the prevalence of asthma in obese people is twice as high as in non-obese people. A meta-analysis of more than 300,000 patients showed an increased risk of asthma with increased body mass index (BMI) (2, 6). A longitudinal American cohort study followed over 4,000 participants for 25 years and showed that BMI strongly predicted asthma in females (7). Another large-scale Norwegian population-based study involving more than 23,000 adults revealed the relationship between the incidence of asthma and metabolic syndrome in which obesity is a major component, regardless of sex, allergic rhinitis, and atopic status (5). In addition, some studies have suggested an association between childhood obesity and the development of asthma (8). A longitudinal study conducted in the United States reported that early childhood asthma increased the risk of obesity later in childhood or adolescence (9). Moreover, increased BMI was associated with increased severity of asthma, resistance to inhaled corticosteroids, increased hospitalization, and impaired quality of life among asthmatic patients (6, 10). Concerning lung function, obese individuals showed a slight decrease in forced expiratory volume in a second (FEV1) and forced vital capacity (FVC) (11, 12).

Airway hyperresponsiveness (AHR), an excessive airway constriction in response to stimuli, is a major feature of asthma and can be found in otherwise healthy individuals (13). Asymptomatic AHR is clinically important because it is a risk

factor for developing asthma (14). Obesity has been shown to be associated with AHR after adjusting potential confounders (1, 15). In a longitudinal follow-up of middle-aged adults, each increase in the BMI of 1 kg/m^2 was associated with a 5% increase in the odds of AHR (odds ratio [OR] 1.05, 95% confidence interval [CI] 1.01–1.09) (16). A longitudinal study on the association between AHR occurrence and BMI with a 4-year follow-up showed that an initial high BMI was associated with AHR development (17). Interestingly, an initial low BMI also increased the risk for the AHR development in this study, which appeared to be partly mediated by weight gain (17). Obesity is referred to abnormal or excessive fat accumulation and is usually defined by BMI, calculated by normalizing an individual's body weight to their height (kg/m^2) (18). However, BMI is calculated from total body weight, which is composed of fat mass (FM) and muscle mass (MM). In addition, MM and FM compositions change over time independently (19). Studies have reported that changes in FM and MM differentially affected lung function in otherwise healthy individuals (20). Therefore, it is relevant to focus on the FM change over time in evaluating obesity's effect on the AHR development.

Several experimental models have been used to study the underlying mechanisms associated with asthma and obesity. High-fat diet (HFD)-fed AKR mice showed a lower threshold of allergen sensitization, increased pro-inflammatory macrophages, increased levels of serum interleukin (IL)-6, and airway eosinophilia, and these positively correlated to increased body weight (21). HFD-fed C57BL/6 mice challenged with ovalbumin presented with increased eosinophils in the lung tissue and increased inflammatory cytokines such as IL-5, tumor necrosis factor-alpha (TNF-α), and IL-10 in bronchoalveolar lavage (BAL) fluid compared to lean mice

(22). Moreover, house dust mite-sensitized HFD-fed C57BL/6J mice showed also increased eosinophils in their BAL and increased ILC2s and ILC3s (23). The results of above studies may be due to the difference in the mice type and sensitization.

It has been reported that increased leptin in obese mice was associated with exacerbation of allergic asthma and increased AHR (24, 25). A previous study suggested that augmented type 2 innate lymphoid cells (ILC2s), alternatively activated macrophages (M2), adipokine disbalance (increased leptin and decreased adiponectin), and increased TNF-α, interferon (IFN)-γ, IL-1β, IL-6, IL-17, and IL-33 as possible underlying mechanisms of AHR (26). In addition, mitochondria dysfunction, microbial dysbiosis, and gut-driven antigens, and so-called "metabotypes" such as increased glyoxylate, dicarboxylate, pyruvate, and methane have been suggested to aid in AHR development (27-31). Interestingly, AHR developed in obese mice fed with an HFD without allergic sensitization (32). Therefore, obese HFD-fed mice may represent a model that can be used to study obesity-related AHR.

Classically activated macrophage (M1) and M2 macrophage alterations in obesity have been suggested based on the notion that the white adipose tissue (WAT) of obese animals showed predominant infiltration of M1 whereas that of lean animals included mainly M2 macrophages (33, 34). Although it may be an oversimplified dichotomy, it is currently believed that M1 macrophages produce pro-inflammatory cytokines, whereas M2 macrophages produce anti-inflammatory cytokines (35). Obesity is a chronic inflammatory disease involving multiple cell types, and to date, enhanced M1 macrophage polarization has been suggested in obesity as well as other inflammatory diseases such as sepsis, atherosclerosis, rheumatoid arthritis, and

diabetes (33, 36). Obesity has been shown to cause an imbalance in the polarization and distribution of macrophages (35, 37). For example, WAT resident cells from lean mice included less than 10% M2 macrophages, whereas WAT resident cells from obese mice included up to 50% M1 macrophages (35, 37). Prolonged HFD caused adipocytes to produce TNF-α, free fatty acids (FFAs), and some chemokines, which recruited monocytes in circulation into WAT. These monocytes were converted to M1 macrophages and induced inflammation by the secretion of pro-inflammatory cytokines, such as TNF-α, IL-1β, and IL-6 (33, 38).

Diet-induced obesity promoted T helper 17 (Th17) differentiation in adipose tissue, and in the airways of obese individuals, IL-17 was secreted by Th17 stimulated type 3 innate lymphoid cells (ILC3s) (39). IL-1β also promoted the secretion of IL-17 in ILC3s (32, 40). ILCs do not express antigen-specific receptors; instead, they respond to cytokines secreted by surrounding cells, such as macrophages, dendritic cells, and epithelial cells (41). ILCs are classified by type according to their cytokine production and developmental pathways: type 1 ILCs produce IFN-γ, type 2 produce IL-5 and IL-13, and type 3 produce IL-17 and IL-22 (42). In previous studies, IL-1β^+ M1 macrophages and ILC3s were increased in the lungs of obese asthmatic mice, and suggested that these cells may have roles in the development of obesity-related asthma (32, 43).

It is well known that there is intimate crosstalk between metabolism and the immune system, often referred to as immunometabolism (44). Glutamine is an essential fuel for cells and modulates the function of leukocytes, macrophages, and lymphocytes (45, 46). Interestingly, it was reported that glutamine was the most markedly reduced polar metabolite in obesity based on metabolomic analyses of

WATs (47). The M2 macrophage population is reduced in the absence of glutamine since glutamine promotes the differentiation of M2 macrophages via the induction of the glutamine-UDP-N-acetylglucosamine (GlcNAc) pathway and the production of α-ketoglutarate (α-KG) (35). Obese individuals showed altered glutamine metabolism with increased levels of glutamate and glutamate/glutamine ratio, possibly due to increased activity of glutaminase, an enzyme that converts glutamine to glutamate (Fig. 1) (48, 49). Decreased levels of glutamine synthetase (GS), which converts glutamate to glutamine, and glutamate dehydrogenase (GDH), which converts glutamate to α-ketoglutarate, also resulted in increased glutamate (48, 49). Moreover, glutamine links obesity to inflammation in human WAT (50). However, there is a lack of research on the link between glutamine metabolism and immune cells related to obesity-induced AHR.

This study aims to elucidate the mechanism of AHR development in obesity. First, the role of FM, instead of BMI, as a risk factor for developing AHR needs to be established. A longitudinal follow-up study is necessary to gain proper insight into the causal relationship between FM and AHR. For these reasons, a health checkup database will be used in this study. The evaluation in healthy individuals will help identify the role of FM, measured by a bioelectrical impedance analysis (BIA), in the development of AHR. The investigation into the mechanisms that underlie obesity-related AHR will be done using a murine obesity model. We will evaluate the changes in glutamine metabolism, and the effects glutamine has on the development of AHR in obese mice on an HFD, particularly focusing on macrophages and ILC3s.

Figure 1. Glutamine metabolism

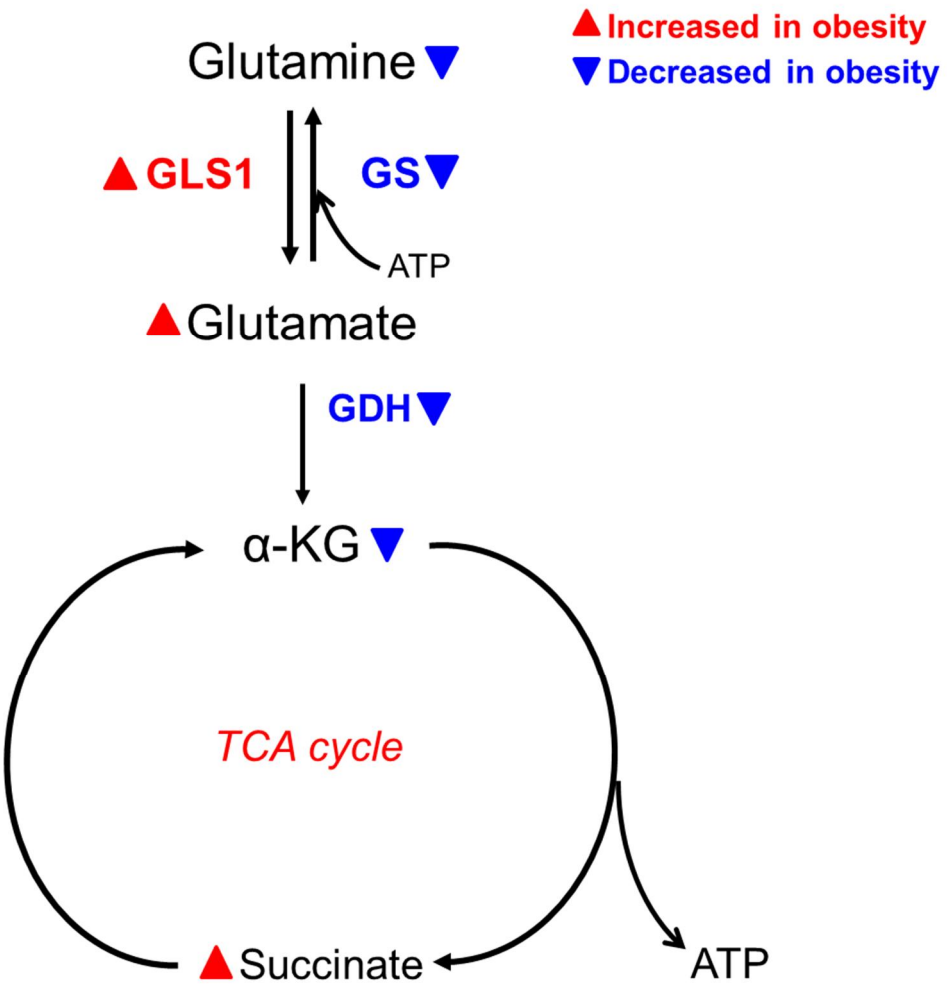

GLS, glutaminase; GS, glutamine synthetase; GDH, glutamate dehydrogenase; α-KG, α-ketoglutarate; TCA cycle, tricarboxylic acid cycle; ATP, adenosine triphosphate.

Part I. Methods

Data source and study population

A long-term longitudinal study deals with subject drop-out, missing values, and incomplete information on variables that affects the development of AHR. In this sense, health checkup databases are of particular interest. Although there is a potential for selection bias, health checkups yield long-term repetitive measurements (without missing data) obtained using uniform standard methods and comprehensive information on comorbidities and confounders (51). The study population was selected from databases from the Seoul National University Hospital Healthcare System Gangnam Center. All individuals were self-recruited for routine health checkups and were usually funded by either private or national health insurance. The database spanned 15 years (October 2004 to May 2019). In a longitudinal analysis, individuals who underwent two methacholine bronchial provocation tests (MBPTs) with a follow-up period of more than three years between the first and second tests were included. Individuals whom self-reported respiratory diseases affecting lung function or AHR, such as asthma, chronic obstructive pulmonary disease (COPD), or pulmonary fibrosis, were excluded. A smoker was defined as an individual with a smoking history of more than ten pack-years; this significantly predicts the development of AHR (52).

The Part I study protocol was approved by the Institutional Review Board of Seoul National University Hospital (H-1601-080-734). The Board waived the need for informed participant consent.

Measurements

Lung function tests were routinely performed in all health checkups using a flow sensing type spirometer (MasterScreen Pneumo; Viasys Respiratory Care, Inc., San Diego, CA, USA), following the American Thoracic Society's recommendations (53). Forced vital capacity (FVC) and forced expiratory volume in one second (FEV1) were measured, and the results were expressed as absolute (mL) and predicted values (%) calculated from a formula based on the Korean population (54). MBPT was performed according to standards (55). FVC and FEV1 were determined after inhaling normal saline and doubling methacholine concentrations in the normal saline solution, and values ranged from 0.5 to 16.0 mg/mL. A Wright twin nebulizer was used to deliver the methacholine solution, inhaled in five tidal breathings. After each dose, FVC and FEV1 were measured after 30 and 90 seconds. At five-minute intervals, doubled methacholine concentrations were given until the FEV1 fell by 20% from the lowest value following saline solution FEV1 or until a dosage of 16 mg/mL was reached. By linear interpolating the last two data points, the provocative concentration of methacholine causing a 20% decrease in FEV1 (PC20) was estimated. The subjects with a 20% or more decline in FEV1 with less than 16 mg/mL methacholine were defined as having AHR.

BIA is a non-invasive technique for assessing body composition and is widely used in routine health checkups. Segmental BIA measures appendicular skeletal MM, and can be used as a proxy for skeletal MM (56). Compared with the reference methods, such as dual-energy X-ray absorptiometry, segmental BIA is a reliable method to measure skeletal MM even in elderly populations (57). Segmental single-frequency BIA measurements were taken (Inbody 720; Biospace Corporation, Seoul,

Korea) of individuals in their bare feet wearing light clothing. Segmental BIA measures the composition of limbs and trunk separately and provides the sum of predicted MM (kg) from the limbs as a proxy for skeletal MM and the whole-body FM (kg). Both MM and FM were normalized by dividing by height (m^2) to generate the MM index (MMI) and FM index (FMI).

Statistical analysis

A cross-sectional analysis of MMI and FMI values with the detection of AHR at the first health checkup was performed. MMI and FMI values were compared between individuals with AHR and those without AHR using paired t-tests and multivariate logistic regression analyses adjusted for age, sex, smoking status, and baseline FEV1 and FVC predicted values were conducted. Correlations between MMI or FMI and PC20 values in individuals with AHR were evaluated. Longitudinal analyses of MMI and FMI annual change rates ([kg/m^2]/year) in each individual were calculated using all measurements obtained over the follow-up period. MMI and FMI change rates were compared between individuals who developed AHR and those who were negative for AHR. All statistical analyses were done using R version 4.0.2 (R Foundation for Statistical Computing, Vienna, Austria), and a two-sided *p*-value less than 0.05 was considered statistically significant.

Part I. Results

Cross-sectional analysis

A total of 4,023 individuals were included in the cross-sectional analysis (1,290 females and 2,733 males). Among them, 112 individuals tested positive for AHR (AHR_{pos}) at the first health checkup. Characteristics measured at the first health checkup are presented in Table 1-1. Mean age, smoker proportion, BMI, and FMI were significantly higher in the AHR_{pos} group than in the AHR negative (AHR_{neg}) group. All lung function measurements, including the FEV1/FVC ratio, were significantly lower in the AHR_{pos} group than in the AHR_{neg} group. In line with previous reports, serum levels of high-sensitivity C-reactive protein (hsCRP) were significantly elevated in the AHR_{pos} group (58-60). A multivariate analysis showed that the risk of having AHR was significantly associated with the FMI values (OR = 1.37, 95% CI: 1.06–1.76, p = 0.017) but not with the MMI values (Table 1-2).

FMI values also showed a significant negative correlation with PC20 values in the AHR_{pos} group (112 individuals) (R = -0.31, p = 0.00087), while MMI values showed no correlation with PC20 values in this group (Fig. 1-1).

Longitudinal analysis

A total of 283 individuals were included in the longitudinal analysis (61 females and 267 males). The mean number of segmental BIA measurements was 6.96 (interquartile range [IQR]: 5–9), and the mean follow-up period was 6.69 years (IQR:

4.63–8.36). Among them, 13 individuals developed AHR (AHR_{pos} conversion group), whereas the others were persistently negative for AHR (AHR_{neg} conversion group). Table 1-3 shows the characteristics of the two groups. Only individuals who were negative for AHR at the first health checkup were included in the longitudinal analysis, and thus all variables except for smoking proportion were similar between the two groups. During the follow-up period, all individuals had gained FM and lost MM. Individuals in the AHR_{pos} conversion group gained more FM than those in the AHR_{neg} conversion group, although the statistical significance was borderline (p = 0.057). Interestingly, differences in the MMI change rate between the AHR_{pos} conversion and AHR_{neg} conversion groups were significant (p = 0.011). Individuals who developed AHR lost significantly more MM compared with the other group.

Next, we conducted multivariate analyses for the risk of a positive conversion of AHR. The risk of developing AHR was significantly associated with an increase in the FMI change rate ([kg/m^2]/year; OR = 1.114x10^4, 95% CI: 1.192–1.551x10^8, p = 0.037) after adjusting for age, sex, smoking, and baseline FEV1 and FVC predicted (Table 1-4).

Table 1-1. Baseline characteristics of all individuals (cross-sectional analysis)

Characteristics	AHR_{neg}	AHR_{pos}	*p*-value
	N=3,911	N=112	
Male, N (%)	2,655 (67.89)	78 (69.54)	NS
Smoker, N (%)	2,122 (54.26)	72 (64.29)	0.035
Age, year	54.04±10.61	57.64±10.90	4.0×10^{-4}
BMI (kg/m^2)	23.70±2.77	24.41±3.21	7.9×10^{-3}
FMI (kg/m^2)	5.91±1.67	6.31±1.97	0.012
MMI (kg/m^2)	9.82±1.45	10.02±1.47	NS
FEV1 (mL)	2,999.73±649.10	2,443.48±563.48	$< 2.0 \times 10^{-16}$
FEV1 predicted value (%)	104.74±13.43	88.88±13.33	$< 2.0 \times 10^{-16}$
FVC (mL)	3,778.82±806.33	3,484.73±800.01	1.4×10^{-4}
FVC predicted value (%)	96.96±11.40	91.56±11.72	8.4×10^{-7}
FEV1/FVC ratio (%)	79.59±6.52	70.56±7.65	$< 2.0 \times 10^{-16}$
hsCRP (mg/dL)	0.12±0.32	0.21±0.27	5.0×10^{-3}

Data are presented as mean±standard deviation. AHR, airway hyperresponsiveness; NS, not significant; BMI, body mass index; FMI, fat mass index; MMI, muscle mass index; FEV1, forced expiratory volume in one second; FVC, forced vital capacity; hsCRP, high-sensitivity C-reactive protein.

Table 1-2. Multivariate logistic analysis for the risk of having AHR (cross-sectional analysis)

Variables	AHR_{pos}	
	OR (95% CI)	*p*-value
Age	1.047 (1.025–1.072)	4.5×10^{-5}
Male	0.179 (0.066–0.475)	6.4×10^{-4}
Smoker	1.822 (0.928–3.710)	NS (0.091)
FMI (kg/m^2)	1.365 (1.057–1.761)	0.017
MMI (kg/m^2)	1.115 (0.968–1.279)	NS
FEV1 predicted (%)	0.835 (0.811–0.858)	$< 2.0 \times 10^{-16}$
FVC predicted (%)	1.119 (1.088–1.152)	1.3×10^{-14}

AHR, airway hyperresponsiveness; OR, odds ratio; CI, confidence interval; FMI, fat mass index; MMI, muscle mass index; FEV1, forced expiratory volume in one second; FVC, forced vital capacity, NS; not significant.

Table 1-3. Characteristics of individuals who developed AHR and those who were persistently negative for AHR (longitudinal analysis)

Characteristics	AHR_{neg} conversion	AHR_{pos} conversion	*p*-value
	N=315	N=13	
Male, N (%)	256 (82.27)	11 (84.61)	NS
Smoker, N (%)	202 (64.13)	12 (92.31)	0.036
Age, year	56.80±8.20	57.92±7.55	NS
Time, year	6.67±2.47	7.36±2.92	NS
BMI (kg/m^2)	24.28±2.76	24.47±2.03	NS
FMI (kg/m^2)	5.92±1.67	5.85±1.14	NS
MMI (kg/m^2)	10.22±1.29	10.44±1.22	NS
FMI change rate ([kg/m^2]/year)	0.0414±0.0609	0.0745±0.0714	NS (0.057)
MMI change rate ([kg/m^2]/year)	-0.0370±0.0343	-0.0618±0.0374	0.011
FEV1 (mL)	3,030.70±585.01	2,930.77±588.73	NS
FEV1 predicted value (%)	104.97±13.79	99.46±13.64	NS
FVC (mL)	3,842.13±712.40	3,857.69±696.11	NS
FVC predicted value (%)	96.93±11.44	94.38±10.90	NS
FEV1/FVC ratio (%)	79.04±6.00	76.32±8.96	NS
hsCRP (mg/dL)	0.15±0.40	0.20±0.33	NS

All except time, FMI, and MMI annual change rates were measured at the first health checkup. Data are presented as mean±standard deviation. AHR, airway hyperresponsiveness; NS, not significant; BMI, body mass index; FMI, fat mass index; MMI, muscle mass index; FEV1, forced expiratory volume in one second; FVC, forced vital capacity; hsCRP, high-sensitivity C-reactive protein.

Table 1-4. Multivariate analysis for the risk of developing AHR (longitudinal analysis)

Variables	AHR_{pos} conversion	
	OR (95% CI)	*p*-value
Age	0.995(0.919–1.076)	NS
Male	0.021(0.001–0.409)	$5.8x10^{-3}$
Smoker	6.636 ($3.307–2.500x10^{3}$)	$9.5x10^{-3}$
FMI change rate ([kg/m^2]/year)	$1.114x10^{4}$ ($1.192–1.551x10^{8}$)	0.037
MMI change rate ([kg/m^2]/year)	$3.471x10^{-10}$ ($1.57x10^{-19}$–0.158)	0.049
FEV1 predicted (%)	0.951 (0.880–1.027)	NS
FVC predicted (%)	1.039 (0.947–1.139)	NS

AHR, airway hyperresponsiveness; OR, odds ratio; CI, confidence interval; FMI, fat mass index; MMI, muscle mass index; FEV1, forced expiratory volume in one second; FVC, forced vital capacity, NS; not significant.

Figure 1-1. Correlation between PC20 and FMI or MMI values in individuals with AHR at the first health checkup (N = 112)

A. FMI

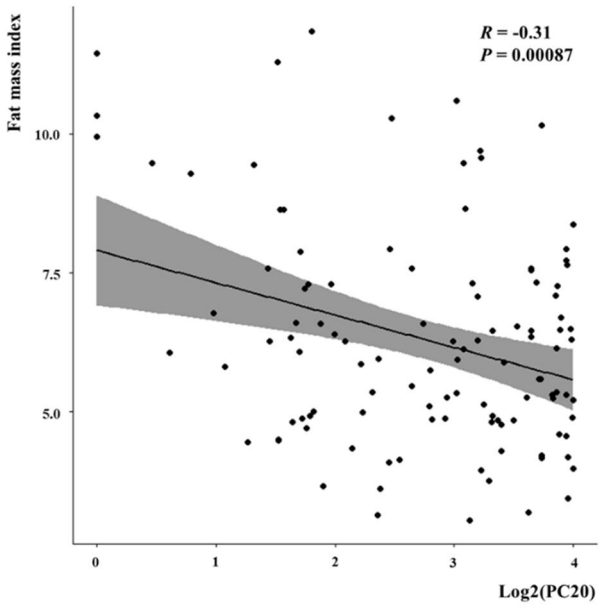

B. MMI

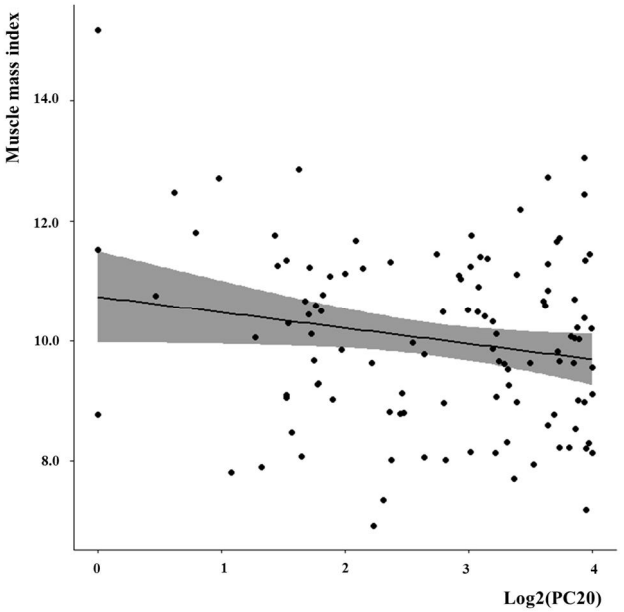

PC20, the provocative concentration of methacholine causing a 20% fall in FEV1; FMI, fat mass index; MMI, muscle mass index; AHR, airway hyperresponsiveness; R, Pearson correlation coefficient.

Part I. Discussion

This study showed that healthy individuals with AHR had significantly greater BMI than those without AHR, which was consistent with previous studies. The difference in BMI was about 0.7 kg/m^2, and is similar to the difference of 1.0 kg/m^2 reported in another study that dealt with AHR in normal people (17). However, this difference in BMI seemed to be caused by differences in FM rather than MM, as FMI values differed significantly between the two groups, but MMI values did not. In addition, FMI values showed a significant negative correlation with PC20 values in individuals with AHR, but MMI values did not show any correlation. Increased FMI, not MMI, was significantly associated with an increased OR for having AHR after adjusting for potential confounders. Individuals with AHR enrolled in this study were a little bit older and had much lower lung function than individuals without AHR. Therefore, these individuals possibly had any hidden diseases that increased their susceptibility of developing AHR, although those who reported respiratory symptoms or respiratory diseases as comorbidities at the first health check-up were excluded from the study. However, a cross-sectional analysis cannot completely exclude the possibility that a gain in FM did not precede all the observed features of individuals with AHR, including lower lung function. In this sense, the results of a longitudinal analysis are of note.

A total of 283 individuals without AHR were followed up for a mean of 6.7 years, and 13 individuals (4.6%) developed AHR. FMI change rates of individuals who developed AHR were higher than those who were persistently negative for AHR;

however, the statistical significance was weak. This means that individuals who developed AHR had gained more FM by about 50 g annually, if height was assumed to be 1.7 m. A small sample size might account for the weak significance. A previous longitudinal study of community-dwelling middle-aged males with a mean follow-up period of 3.74 years found a U-shaped correlation between baseline BMI and AHR development (17). The lowest and the highest quintile of initial BMI showed increased odds ratios for the development of AHR in their study (17). The authors observed that increased BMI every year was prominent in males in the lowest quintile of the initial BMI and developed AHR (17). They suggested that weight gain over the observational period might be associated with an increased risk of developing AHR (17). Body weight is a sum of MM and FM, and it was reported that the rate of change in FMI showed a stronger association with the rate of change in body weight than that of MMI in healthy middle-aged individuals (20). Multivariate analyses of current study showed that an increased FMI change rate, a more rapid gain in FM during the observation time, was significantly associated with the risk of developing AHR. Although the FMI or MMI change rate itself is a small value, and thus the difference between the two groups is small, a previous study showed that an MMI or FMI change rate as small as 0.1 (kg/m^2)/year was associated with an FEV1 decline in healthy individuals (20). Taken together, a gain of FM over time is a risk factor for developing AHR in otherwise healthy individuals.

Another interesting finding of this study was that the loss of MM over time was an important risk factor for developing AHR. With aging, total body FM increases and concomitantly body lean mass and bone density decrease, which is thought to be independent from general and physiological fluctuations in weight and BMI (61).

In addition, obesity and sarcopenia, the loss of MM, are associated with declined lung function (62, 63). Although no association between MMI and AHR was observed in the cross-sectional analysis, as shown in the longitudinal study, a rapid decrease in MMI may be associated with AHR occurrence, and further investigation is needed in this area.

A previous cross-sectional study showed that sarcopenic obesity was associated with lower FEV1 values than sarcopenia alone in male patients with COPD (64). Sarcopenia with obesity is associated with higher levels of metabolic disorder and an increased risk for mortality than obesity or sarcopenia alone (65). Currently, there is no widely accepted definition of sarcopenic obesity; however, it normally refers to a high BMI with sarcopenia, measured via dual X-ray absorptiometry (63). Taken together, sarcopenic obesity may increase the risk of developing AHR than obesity alone in otherwise healthy individuals.

Several mechanisms have been proposed to explain the association between obesity and AHR. Obesity can facilitate small airway closure due to its mechanical effect on airway diameter (66). Increased FM in the chest and abdomen, as seen in obesity, can lead to a smaller tidal volume (67). These features result in compressed airways, may be inducing AHR due to geometric effects, and this is supported by studies that showed the beneficial effects of bariatric surgery on AHR (68). Increased serum and tissue levels of obesity-associated pro-inflammatory adipokines affected the development of AHR by altering pulmonary surfactant structure and function (69). These adipokines are known to contribute to airway inflammation, suggesting obesity may predispose to AHR (70). It is unknown if significant airway inflammation occurred in formerly lean individuals who gained FM in this study.

Another plausible link might be the increased dietary intake, which may be associated with AHR (71). Obese people often have unhealthy diets containing fewer antioxidants and omega-3 fatty acids, which have been shown to be beneficial for lung function (72). This is one of the reasons why the Part II study was focused on glutamine, a dietary component. Metabolomic analyses of WAT revealed that glutamine was the most significantly reduced polar metabolite in obese individuals (47). In addition, exogenous glutamine exhibited potent anti-inflammatory activity against both T helper 1 (Th1) and T helper 2 (Th2) cell-associated allergic lung inflammation in a murine model of asthma (73).

This study had a few limitations. First, individuals included in the study underwent health checkups at only one center, which may have introduced selection bias. Second, the demographic of participants in the study may be a source of selection bias since individuals who engage in unhealthy behaviors, such as smoking, may want to receive additional tests like MBPT. Next, we have no data on serum adipokines, such as adiponectin and leptin, in participants, which are known to be important for pathologic changes caused by obesity. Finally, the small number of participants was an important limitation. These points should considered when generalizing the present study's observations.

Part II. Methods

HFD-fed obese mice and the effect of GLS1 inhibition on AHR

Four-week-old male C57BL/6 mice were purchased from Orient Bio, Inc. (Seoul, Korea). Obesity was induced by feeding mice a diet consisting of 60% kcal of fat (D12492; Research Diets, Inc., New Brunswick, NJ, USA) for 13 weeks, whereas the control group was fed a standard chow diet for the same period (chow group). HFD-fed obese mice were divided into two groups: (1) HFD only (HFD group) and (2) HFD mice that were administered an intraperitoneal injection of 200 μg Bis-2-(5-phenylacetamido-1,3,4-thiadiazol-2-yl)ethyl sulfide (BPTES), a selective inhibitor of glutaminase 1 (GLS1), every three days from day 3 to day 90 (HFD + BPTES group). A BPTES (SelleckChem, Houston, TX, USA) stock solution was prepared by dissolving BPTES in one milliliter of warm dimethyl sulfoxide (Sigma-Aldrich, St Louis, MO, USA), followed by dilution in phosphate-buffered saline. The injection dose and interval of BPTES were selected based on previous reports (74, 75). At 13 weeks, bronchoalveolar lavage fluid (BALF), blood, lung tissue, and epididymal WAT were collected from sacrificed mice. To evaluate AHR, mice were challenged with increasing doses of inhaled methacholine (0, 12.5, 25, 50, and 100 mg/mL, Sigma-Aldrich), followed by the measurement of airway resistance ($cmH_2O/mL/s$) using the forced oscillation technique as previously described (76). We chose the dose of 100 mg/mL of methacholine as the representative result (76).

All experiments were approved by the Institutional Animal Care and Use Committee of the Institute of Laboratory Animal Resources at Seoul National University Hospital (IACUC 20-0265-S1A0).

BALF cells, Serum, lung and adipose tissue analysis

Triglycerides and glucose were measured in the serum with kits from Biovision (Milpitas, CA, USA), and serum leptin and adiponectin were measured with kits from Abcam (Cambridge, MA, USA). Glutamine and glutamate were measured in the serum and lysates from lung and adipose tissues with kits from Biovision (Milpitas, CA, USA). To detect glutamine and glutamate levels in lung and adipose tissue lysates, 40 mg of lung tissue and 100 mg of adipose tissue was homogenized in 0.4 ml ice-cold cell lysis buffer containing protease inhibitor. Tissue homogenates were then incubated on ice for 30 minutes, and the lysates were centrifuged at 12,000 × g for 10 minutes at 4°C. Supernatants were aliquoted and stored at -80°C. Briefly, for detection of glutamine levels, a hydrolysis enzyme was added to the standard and sample (serum; 1:50 dilution, lung and adipose tissue lysates; 1:2 dilution) wells, and then the reaction mix was added after incubation at 37°C for 30 minutes. After additional incubation at 37°C for 60 minutes, the absorbance (OD 450 nm) was measured. To detect glutamate levels, the reaction mix was added to the same samples as above, and the absorbance (OD 450 nm) was measured after incubating at 37°C for 30 minutes. Preparations of BALF cells were prepared on slides and stained with Diff-Quick (Sysmex International Reagents, Kobe, Japan) for the analysis of cell counts.

Histopathology

To evaluate and compare the severity and character of pathological changes in lung parenchyma and adipose tissue, left lung and adipose tissue of mice were fixed in 10% neutral buffered formalin and embedded in paraffin, 3-mm sections were stained with hematoxylin and eosin (H&E). Lung tissue was also stained with Masson trichrome.

Cell analysis by flow cytometry

We analyzed ILC3s, Th1 and Th17 cells from mouse lung tissue. M1 and M2 macrophages were analyzed from lung tissue and WAT from mice. For fluorescence-activated sorting of these cells, the following antibodies were used: allophycocyanin (APC)-conjugated retinoic acid receptor-related orphan receptor γt (RORγt), BV506-conjugated anti-F4/80, PE/cy7-conjugated anti-pro-IL-1β, AF564 or AF647-conjugated anti-goat IgG (Thermo Fisher Scientific, Waltham, MA, USA), BV605-conjugated anti-CD127 (IL-7R), BV711-conjugated anti-CD4, BV421-conjugated anti-IL-17A, FITC-conjugated anti-CD11b (BioLegend, San Diego, CA, USA), APC/cy7-conjugated anti-CD11c (BD Biosciences, San Jose, CA, USA), and anti-CD206 (R&D Systems, Minneapolis, MN, USA). PE-conjugated anti-arginase-1 (Arg-1) (R&D Systems, Minneapolis, MN, USA) and anti-CD206 (R&D Systems). For ILCs, lineage-negative cells (Lin^-), $CD3^-$, $CD4^-$, $CD8^-$, $CD11b^-$, $CD11c^-$, $CD19^-$, $F4/80^-$, $Fc\varepsilon RI^-$, and $CD49b^-$, were sorted using CD127 as a surface marker (77). ILC3s were defined as $CD45^+Lin^-CD127^+ROR\gamma t^+$ lymphoid cell populations. Th1 and Th17 cells were defined as $CD4^+T\text{-}bet^+$ and $CD4^+IL\text{-}17A^+$ cells, respectively.

M1 macrophages were gated for $CD11b^{+}CD206^{-}CD11c^{+}$, and M2 macrophages were gated for $CD11b^{+}CD206^{+}CD11c^{-}$. Flow cytometry was performed using BD LSRFortessa™ and BD LSRFortessa™ X-20 (BD Biosciences), and the results were analyzed using the FlowJo software (version 10.2; BD Biosciences).

Effect of GLS1 inhibition on the induction of M1 or M2 macrophages in vitro from BMDM or a mouse alveolar macrophage cell line

Upregulation of toll-like receptor 4 (TLR4) expression and subsequent downstream activation of the nucleotide-binding domain (NOD)-like receptor protein 3 (NLRP3) inflammasome are important steps in IL-1β responses of M1 macrophages (32, 78, 79). To investigate the influence of changes in glutamine metabolism on the TLR4-NLRP3 pathway, we performed additional in vitro experiments using bone marrow-derived macrophages (BMDMs) from naïve mice and a murine alveolar macrophage cell line.

BMDMs from a seven-week-old male C57BL/6 naïve mouse were prepared using the previously described methods (80). Mature BMDMs were detected by identifying $CD11b^{+}$ cells on day seven and then stimulated with lipopolysaccharide (LPS) (100 ng/mL, Sigma-Aldrich) to induce M1 macrophage polarization. LPS-induced M1 macrophages were treated with either three micromoles of BPTES (LPS + BPTES group) or two millimoles of L-glutamine (Sigma-Aldrich) (LPS + glutamine group) (81, 82). We measured the population of TLR4-expressing pro-IL-$1\beta^{+}$ cells in four groups of BMDMs: 1) BMDMs, 2) LPS-induced M1 macrophages,

3) LPS-induced M1 macrophages treated with BPTES, and 4) LPS-induced M1 macrophages treated with glutamine.

AMJ2-C11 (CRL-2456™), a mouse alveolar macrophage cell line, was purchased from American Type Culture Collection (ATCC, Manassas, VA, USA). The cells were stimulated by either LPS for M1 macrophage polarization or IL-4 and IL-13 (both at 10 ng/mL; Thermo Fisher Scientific) for M2 macrophage polarization, and they were cultured with three micromoles of BPTES or 2 millimoles of glutamine. Next, the expressions of TLR4, pro-IL-1β, NLRP3, CD206, and Arg-1 in $CD11b^+$ cells were detected using flow cytometry in each group.

Effect of GLS1 inhibition on the IL-17-producing ILC3s differentiated from ILCs in vitro in the naïve mouse lung

Previously, it was suggested that the NLRP3-IL-1β-ILC3-IL-17A axis plays a crucial role in HFD-induced AHR (32, 83). Thus, this study examined the effects of BPTES or glutamine treatment on the IL-17-producing ILC3s differentiated from ILCs in vitro in the naïve mouse lung.

ILCs (5×10^4 cells/well) which were gated as $CD45^+Lin^-CD127^+$ cells from lung tissue of naïve mice (n = 10), and were stimulated with IL-2 (10 ng/mL; R&D Systems), IL-7 (10 ng/mL; R&D Systems), IL-1β (20 ng/mL; Biolegend), and IL-23 (20 ng/mL; Thermo Fisher Scientific) for ten days to induce ILC3 differentiation. ILC3s were incubated with three micromoles of BPTES or two millimoles of glutamine, followed by intracellular staining for RORγt and IL-17A. ILC3s were stimulated with phorbol myristate acetate (PMA) (100 ng/mL), ionomycin (1 μg/mL),

and GolgiStop four hours before cell harvesting and were then stained with PE/cy7-conjugated anti-IL-7R. Finally, these cells were permeabilized using the Cytofix/Cytoperm kit (BD Biosciences) and incubated with APC-conjugated anti-RORγt and BV421-conjugated anti-IL-17A.

Glutamine and glutamate levels and glutamate to glutamine ratio in human samples

We collected plasma samples from obese or non-obese individuals without a history of asthma (control) who visited the Seoul National University Hospital for health screening between September and November 2021. The control group met the following criteria: adults aged 19 years or older, no previous history of asthma and smoking, predicted FEV1 greater or equal to 80% and FEV1/FVC greater than or equal to 70%, and non-atopic, negative for skin prick test for inhalant allergens. Thus, we included obese (n = 14) and non-obese (n = 10) controls. The study protocol was approved by the Institutional Review Board of the Seoul National University Hospital (H-2107-149-1237), and informed consent was obtained from all participants. We also obtained plasma samples from 14 obese and 17 non-obese asthmatics from the Biobank of Soonchunhyang University Hospital, Bucheon, South Korea. The diagnosis of asthma was as follows; 1) the presence of one or more of the following symptoms: dyspnea, cough, or wheezing, and 2) proven AHR or airway reversibility. AHR was determined as positive when PC20 was less than 16 mg/mL in an MBPT, and airway reversibility was defined as an increase in FEV1 at least 12% from the baseline after inhalation of 400 μg of salbutamol or four weeks

of anti-inflammatory treatment with systemic or inhaled corticosteroids. We enrolled non-smokers and former smokers with a smoking history of less than ten pack-years. Obesity was defined as a BMI of at least 25 kg/m^2 according to the Asia-Pacific classification of BMI (84). We estimated the plasma levels of glutamine (1:10 dilution), glutamate (1:10 dilution), IL-1β (1:5 dilution), and IL-17 (1:5 dilution, BioLegend) in human blood samples from the following four groups: 1) non-obese individuals without asthma (normal control); 2) obese individuals without asthma (obese control); 3) obese and non-atopic asthmatics (obese asthmatics); and 4) non-obese and non-atopic asthmatics (non-obese asthmatics).

Statistical analysis

Data were analyzed for significance using a one-way analysis of variance with Bonferroni post-test correction for multiple comparisons. *P-values* less than 0.05 indicated statistical significance. Statistical analyses were performed using the GraphPad Prism 9.0.1 software (GraphPad Software, La Jolla, CA, USA).

Part II. Results

Increased serum and lung glutamate to glutamine ratio in HFD-fed obese mice

In the serum and lung tissue lysate, the HFD group showed significantly higher levels of glutamine and glutamate and increased glutamate/glutamine ratio compared to the chow group ($p < 0.05$), which significantly decreased after treatment with BPTES ($p < 0.05$) (Fig. 2-1A and B). Likewise, in the adipose tissue lysate, glutamine and glutamate levels significantly increased in the HFD group ($p < 0.05$) (Fig. 2-1C). However, these levels were not reduced by BPTES (Fig. 2-1C). Increased glutamate to glutamine ratio indicates an enhanced conversion of glutamine to glutamate through GLS1.

GLS1 inhibition attenuated AHR and airway inflammation in HFD-fed obese mice

The baseline characteristics of the chow, HFD, and HFD + BPTES groups are shown in Table 2-1. The HFD group displayed a significantly higher mean body weight (47.9 ± 3.1 vs. 36.5 ± 0.8 g, $p < 0.01$), epididymal fat pad weight (0.9 ± 0.1 vs. 0.6 ± 0.1 g, $p < 0.05$), and serum levels of glucose, triglycerides, and leptins compared to the chow group ($p < 0.05$) (Table 2-1). The numbers of inflammatory cells in the BALF, including macrophages ($p < 0.01$), neutrophils ($p < 0.05$), and

lymphocytes ($p < 0.01$), were significantly higher in the HFD group than those in the chow group (Table 2-1). AHR developed in the HFD group, and histology results showed increased inflammatory cells, including macrophages and neutrophils, and collagen deposition in the airways and WAT (Fig. 2-2A and B). However, the HFD + BPTES group displayed significantly lower counts of macrophages and lymphocytes in the BALF ($p < 0.05$) (Table 2-1), attenuated AHR ($p < 0.05$), and less inflammatory cell deposition in the histologic examination compared to the HFD group (Fig. 2-2A and B).

GLS1 inhibition attenuated the increase of ILC3 and IL-1β$^+$ M1 macrophages in the lung of HFD-fed obese mice

Levels of ILC3s, Th1 and Th17 cells in lung tissue were investigated using antibodies against CD127, RORγt, T-bet, and IL-17 (Fig. 2-3A). ILC3s were significantly increased in the HFD group compared to those in the chow group, but this increase was reduced significantly by BPTES ($p < 0.01$) (Fig. 2-3B). However, Th1 and Th17 cells showed no differences between the groups (Fig. 2-3B).

Next, macrophages in lung and adipose tissues focusing on pro-IL-1β expression in M1 macrophages were examined since it was reported that HFD-activated IL-1β-secreting M1 macrophages caused ILC3s to secrete IL-17 and induced AHR (32). Based on the previous reports showing that CD11b$^+$CD11c$^+$ cells increased in the lung tissue with inflammatory conditions (85, 86), cell populations were divided according to their expression levels of CD11b and CD11c (Fig. 2-4A). In the HFD group, CD11b$^+$CD11c$^+$ cells significantly increased compared to the chow group but showed

no difference compared with the HFD + BPTES groups (Fig. 2-4A and B). However, the high population of CD11b and CD11c cells showed no difference among groups (Fig. 2-4A and B). The frequency of pro-IL-1β-expressing M1 macrophages, pro-IL-1β^{+}CD206^{-} cells in the CD11b^{+}CD11c^{+} cell population, also significantly increased in the HFD group but was significantly attenuated in the HFD + BPTES group ($p < 0.05$) (Fig. 2-4B). Meanwhile, pro-IL-1β^{+}CD206^{-} cells were rarely observed in the high population of CD11b and CD11c cells (Fig. 2-4A).

In the adipose tissue, M1 macrophages, CD206^{-}CD11c^{+} cells in the CD11b^{+} cell populations, were significantly increased, and M2 macrophages, CD206^{+}CD11c^{-} cells in the CD11b^{+} cell populations, were significantly decreased in the HFD group compared with those in the chow group ($p < 0.01$) (Fig. 2-5A and B). These changes were not affected by treatment with BPTES (Fig. 2-5A and B). A significant increase was observed in pro-IL-1β-expressing M1 macrophages in the HFD group ($p < 0.01$), which was significantly attenuated in the HFD + BPTES group ($p < 0.05$) (Fig. 2-5A and B).

GLS1 inhibition reduced TLR4 and NLRP3 expressions in pro-IL-1β^{+} M1 macrophages induced in vitro by LPS

The population of TLR4-expressing pro-IL-1β^{+} cells in four groups of BMDMs was measured (Fig. 2-6A). First, it was found that the increased glutamate to glutamine ratio in the lysate of LPS-induced M1 macrophages was significantly reduced by treatment with BPTES or glutamine supplementation ($p < 0.05$) (Fig. 2-6B). Next, the frequency of TLR4^{+}pro-IL-1β^{+} cells was significantly higher in LPS-induced M1

macrophages compared to the control group but was significantly lowered by BPTES or glutamine ($p < 0.01$) (Fig. 2-6C).

The gate strategies for M1 and M2 macrophages induced from the murine alveolar macrophage cell line were presented in Fig. 2-7A. $CD206^{+}Arg\text{-}1^{+}$ is a known marker for IL-4/IL-13-induced M2 macrophages (87). The glutamate to glutamine ratio was significantly reduced by BPTES or glutamine in the lysate of LPS-induced M1 macrophages (Fig. 2-7B). However, a significant reduction of the glutamate to glutamine ratio in the lysate of IL-4/IL-13-induced M2 macrophages was observed only in the glutamine group (Fig. 2-7B). The $NLRP3^{+}TLR4^{+}pro\text{-}IL1\beta^{+}$ cells in the LPS-induced M1 macrophages significantly decreased when treated with BPTES or glutamine ($p < 0.01$) (Fig. 2-7C). Meanwhile, IL-4/IL-13-induced M2 macrophages significantly increased when treated with glutamine ($p < 0.01$) but not with BPTES (Fig. 2-7C).

GLS1 inhibition reduced IL-17 production in ILC3s differentiated from ILCs in the naïve mouse lung in vitro

ILCs were sorted from naïve mice lung cells (Fig. 2-8A) and stimulated with rIL-2, rIL-7, rIL-1β, and rIL-23 and induced ILC3 differentiation, followed by treatment with BPTES or glutamine (Fig. 2-8B). The numbers of IL-17-producing ILC3s gated with $ROR\gamma t^{+}IL\text{-}17^{+}$ significantly decreased when treated with BPTES or glutamine ($p < 0.05$) (Fig. 2-8B and C).

Plasma glutamate to glutamine ratio increased in obese asthmatics

The glutamate to glutamine ratio significantly increased in both obese controls ($p < 0.05$) and obese asthmatics ($p < 0.01$) compared to normal controls, but the magnitude and statistical significance in obese asthmatics were slightly higher (Fig. 2-9A). In addition, plasma levels of IL-17 and IL-1β were significantly elevated in obese asthmatics compared to normal controls (Fig. 2-9B and C).

Table 2-1. The laboratory findings of bronchoalveolar lavage fluid and blood in each mouse group

	Chow diet	HFD	HFD + BPTES
Body weight (g)	36.5±0.8	48.0±3.1**	46.6±2.8
Epididymal fat weight (right, g)	0.6±0.1	0.9±0.1*	1.0±0.2
Serum			
Triglycerides (nmol/μL)	1.8±0.0	2.4±0.3*	2.1±0.3
Glucose (nmol/μL)	104.3±16.0	128.3±2.7**	119.2±8.1
Leptin (ng/mL)	1.4±0.2	4.7±0.6**	3.8±0.7*
Adiponectin (μg/mL)	3.5±0.3	2.4±0.7	2.9±1.5
BALF cell count			
Macrophages (/mL)	26,225±9277.6	63380±7816.8**	34,575±4462.0**
Neutrophils (/mL)	725±221.7	2060±805.0*	1,225±287.2
Lymphocytes (/mL)	550±191.5	2560±512.8**	1,700±383.0*

Data are presented as mean±standard deviation. To obtain *p*-value, the HFD group was compared to the chow diet group and the HFD+BPTES group was compared to the HFD group. *$p < 0.05$ and **$p < 0.01$. HFD, high-fat diet; BPTES, GLS 1 inhibitor; BALF, bronchoalveolar lavage fluid.

Table 2-2. Baseline demographics of human subjects enrolled

	Non-obese individuals N=10	Obese individuals N=14	Non-obese asthmatics N=17	Obese asthmatics N=14
Age (year)	53.5±13.6	48.4±13.4	54.1±12.2	62.5±13.2
Sex (male, n)	1	8	9	8
BMI (kg/m^2)	21.6±1.0	28.6±2.1	21.3±2.0	30.0±2.4
Total IgE (IU/mL)	NA	NA	30.4±31.8	44.8±55.7

Data are presented as mean±standard deviation. N, number; BMI, body mass index; IgE, immunoglobulin E; NA, not available.

Figure 2-1. The effects of an HFD and GLS1 inhibition on glutamine and glutamate levels and glutamate to glutamine ratio in mouse serum, lung and adipose tissue

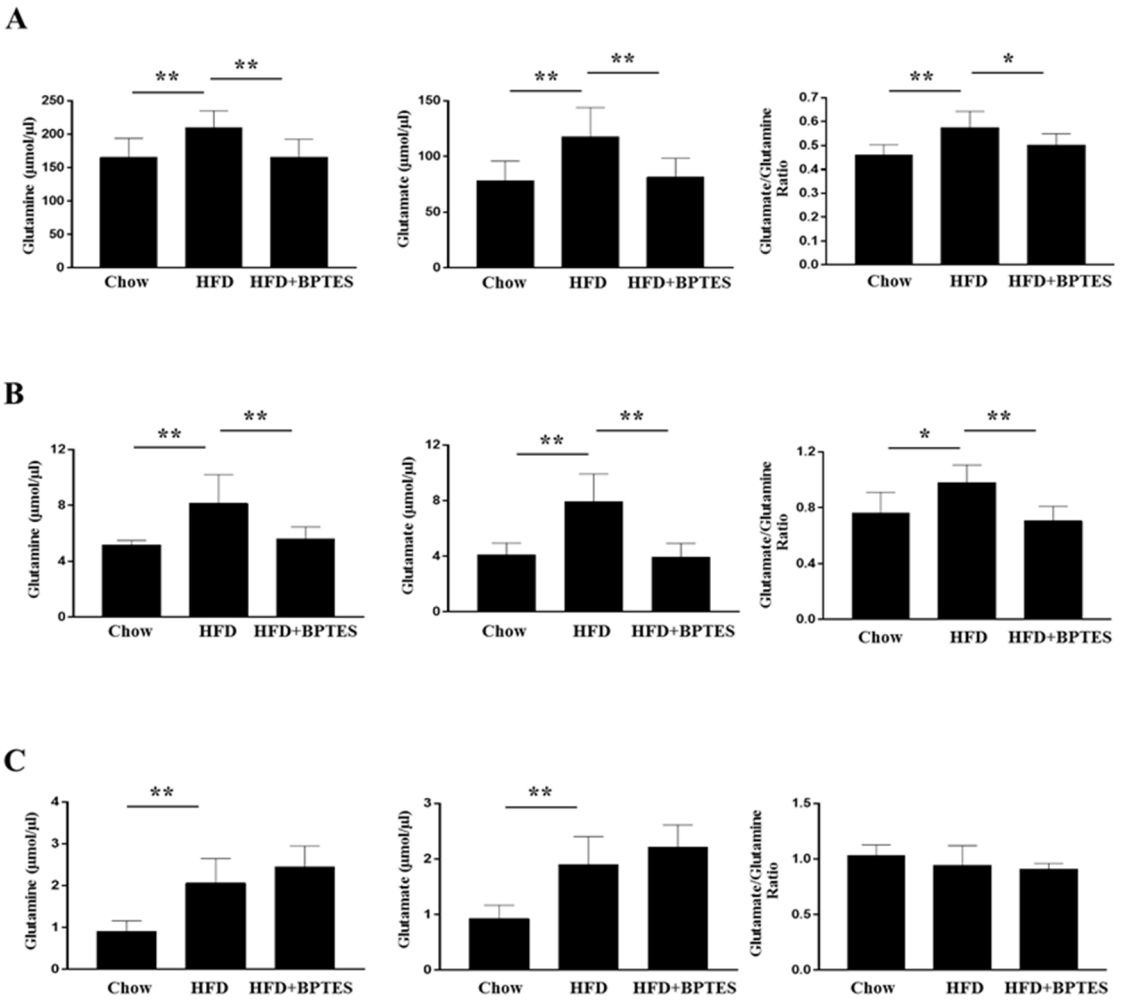

A, Serum. B, Lung tissue lysate. C, Adipose tissue lysate. For the HFD + BPTES group, changes were evaluated 24 hours after the last administration of the GLS1 inhibitor (each group with n = 5–7). $*p < 0.05$, $**p < 0.01$. Statistical analysis determined by one-way ANOVA with Bonferroni's multiple comparisons test. Chow, normal chow diet; HFD, high-fat diet; BPTES, GLS1 inhibitor.

Figure 2-2. The effect of an HFD and GLS1 inhibitor on AHR and inflammation in each group

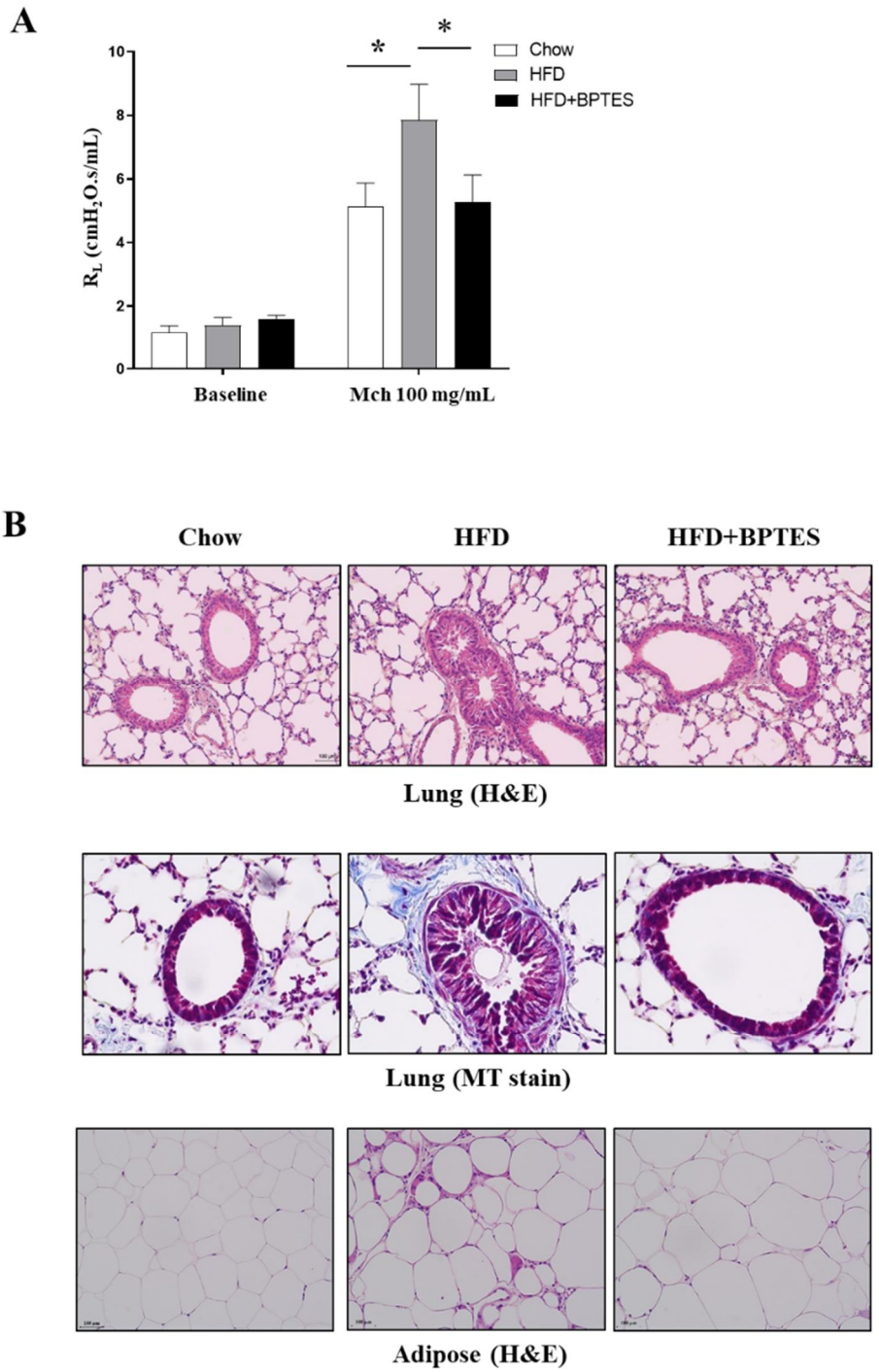

A, Methacholine-induced AHR in each group (Y-axis represents $cmH_2O/mL/s$). B, Histological examination of the mouse lung (*H&E stain,* ×200*; Masson's trichrome stain,* ×400) and adipose tissue (*H&E stain*, ×200) in each group. All scale bars represent 100 μm. $*p < 0.05$. Statistical analysis determined by one-way ANOVA with Bonferroni's multiple comparisons test. HFD, high-fat diet; BPTES, GLS1 inhibitor; Chow, normal chow diet; Mch, methacholine; R_L, airway resistance; H&E, hematoxylin and eosin; MT, Masson's trichrome.

Figure 2-3. The effect of an HFD and GLS1 inhibition on the population of ILC3s, Th1 and Th17 cells in mouse lung tissue

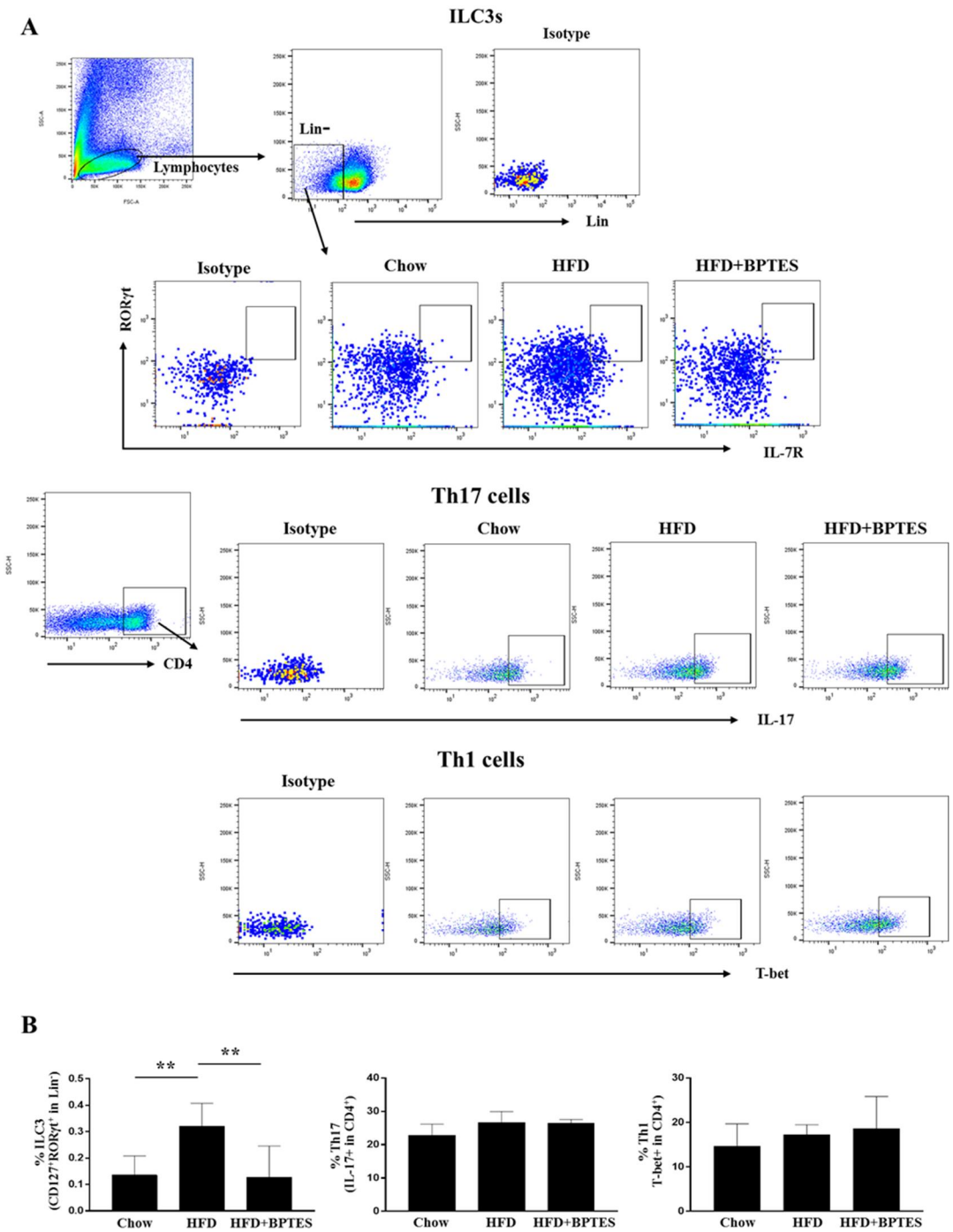

A, Representative gaiting strategy of $CD127^{+}ROR\gamma t^{+}$ ILC3s, $CD4^{+}IL\text{-}17^{+}$ Th17 cells and $CD4^{+}T\text{-}bet^{+}$ Th1 cells in each group. B, Frequencies of ILC3s, Th1 cells and Th17 cells in mouse lung tissue. $^{**}p < 0.01$. Statistical analysis determined by one-way ANOVA with Bonferroni's multiple comparisons test. ILC3; type 3 innate lymphoid cell, Th1; T helper type 1, Th17; T helper type 17, Chow; normal chow diet, HFD; high fat diet, BPTES; GLS1 inhibitor.

Figure 2-4. The effect of an HFD and GLS1 inhibition on the population of macrophages in mouse lung tissues

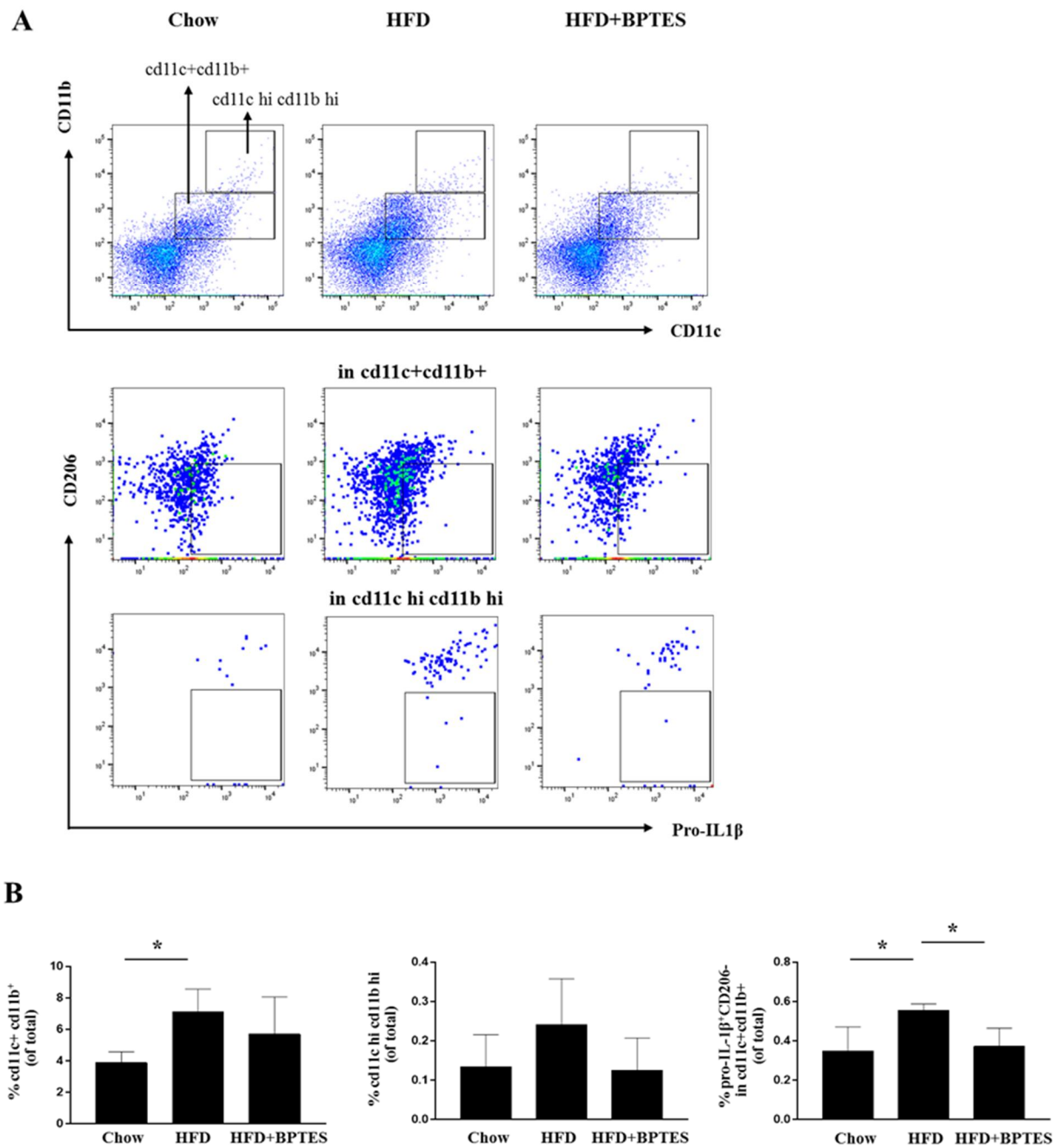

A, Representative gaiting strategy of pro-IL-1β-expressing M1 macrophages (pro-IL1β^{+}CD206^{-} cells in CD11c^{+}CD11b^{+} cells or CD11c hi CD11b hi cells) in mouse lung tissue. B, Frequencies of CD11c^{+}CD11b^{+} cells, CD11c hi CD11b hi cells, and pro-IL-1β-expressing M1 macrophages (pro-IL1β^{+}CD206^{-} cells in CD11c^{+}CD11b^{+} cells) in each group. *$p < 0.05$ and **$p < 0.01$. Statistical analysis determined by one-way ANOVA with Bonferroni's multiple comparisons test. Chow; normal chow diet, HFD; high fat diet, BPTES; GLS1 inhibitor.

Figure 2-5. The effect of an HFD and GLS1 inhibition on the population of macrophages in mouse adipose tissues

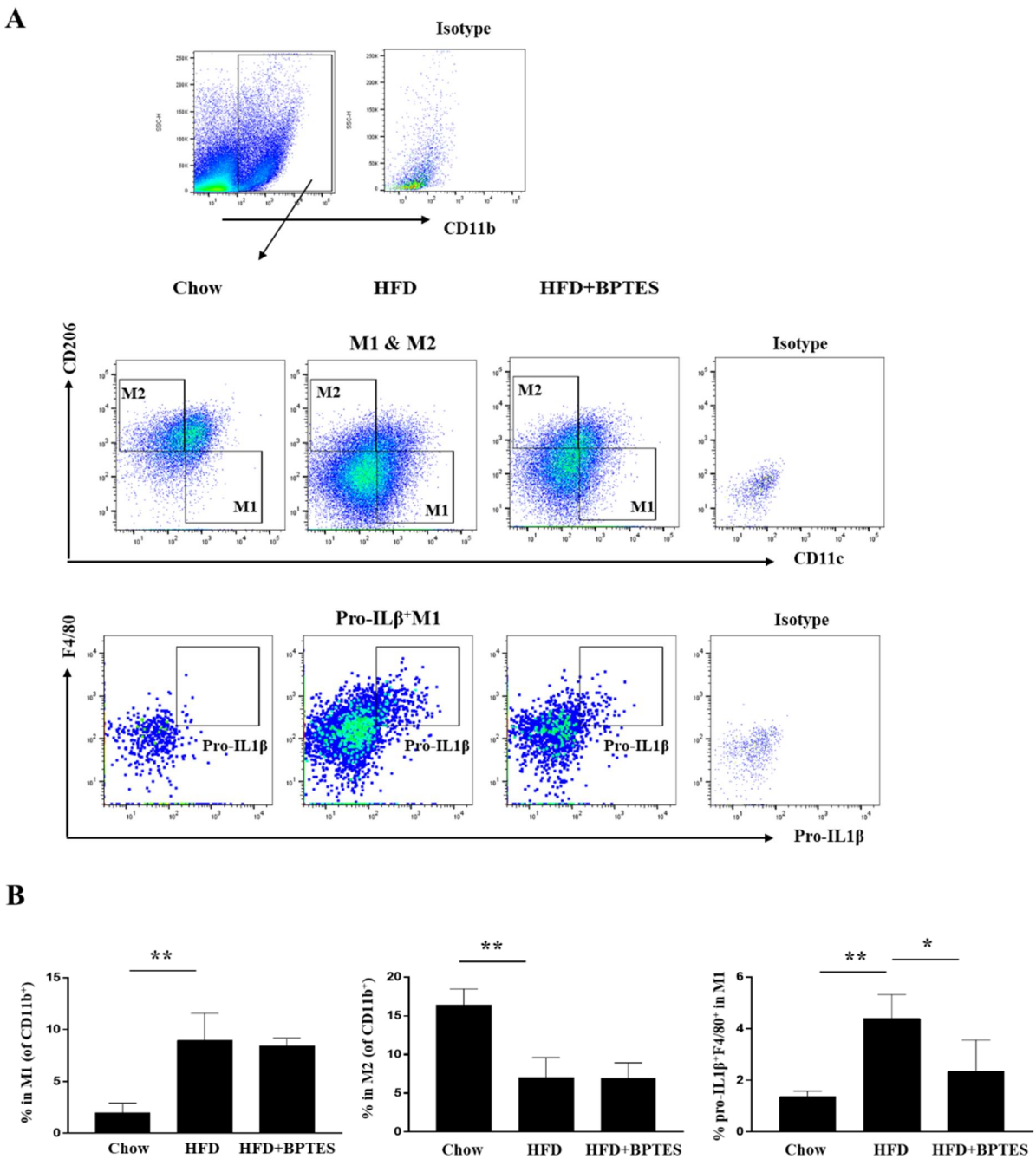

A, Representative gaiting strategy of M1 macrophages ($CD11c^{+}CD206^{-}$) and M2 macrophages ($CD11c^{-}CD206^{+}$) in $CD11b^{+}$ cells and pro-IL-1β^{+}F4/80^{+} M1 macrophages in mouse adipose tissue. B, Frequencies of M1 and M2 macrophages and pro-IL-1β^{+}F4/80^{+} M1 macrophages in each group. *$p < 0.05$ and **$p < 0.01$. Statistical analysis determined by one-way ANOVA with Bonferroni's multiple comparisons test. Chow; normal chow diet, HFD; high fat diet, BPTES; GLS1 inhibitor.

Figure 2-6. The effect of GLS1 inhibition and glutamine supplementation on LPS-induced M1 macrophages originating from BMDMs in vitro

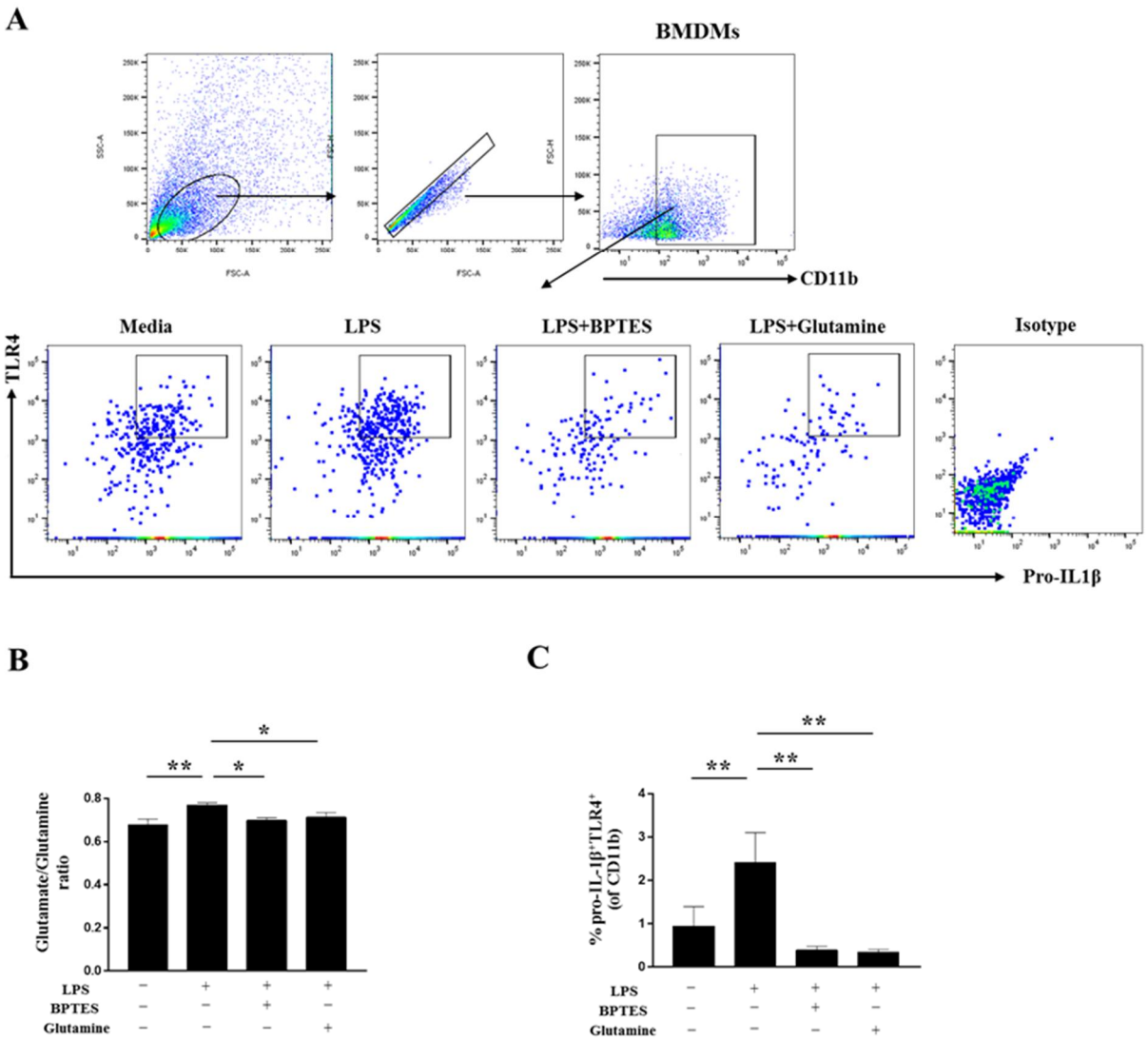

A, Representative gaiting strategy of TLR4^{+}Pro-IL-1β^{+} M1 macrophages originated from BMDMs. B, Glutamate to glutamine ratio in the cell lysate of each group. C, Frequencies of TLR4^{+}Pro-IL-1β^{+} M1 macrophages originating from BMDMs in each group. *$p < 0.05$ and **$p < 0.01$. Statistical analysis determined by one-way

ANOVA with Bonferroni's multiple comparisons test. BMDM; Bone marrow-derived macrophage, LPS; lipopolysaccharide, BPTES; GLS1 inhibitor, TLR4; toll-like receptor 4.

Figure 2-7. The effect of GLS1 inhibition and glutamine supplementation on LPS-induced M1 macrophages and IL-4/IL-13-induced M2 macrophages originating from an alveolar macrophage cell line in vitro

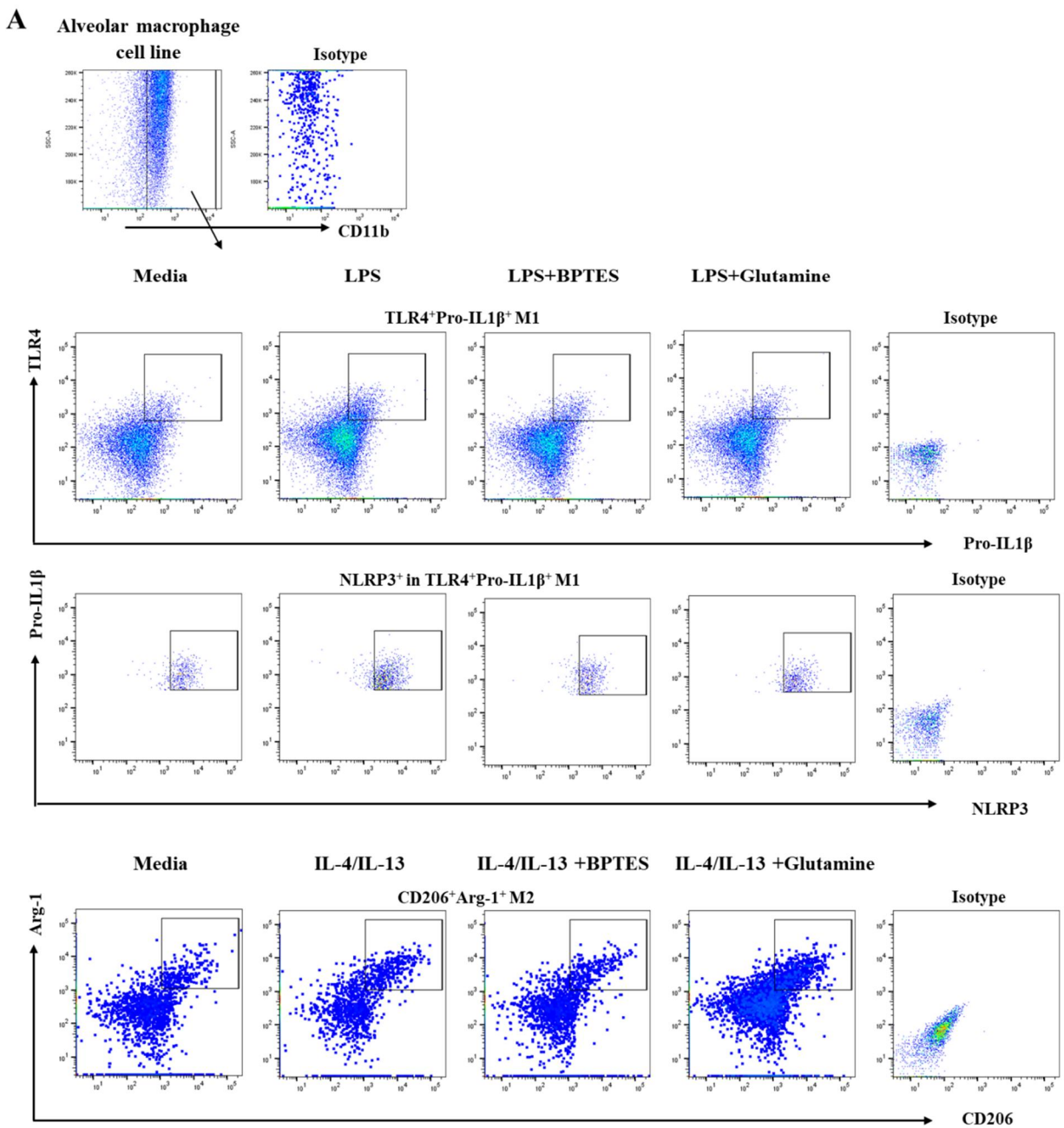

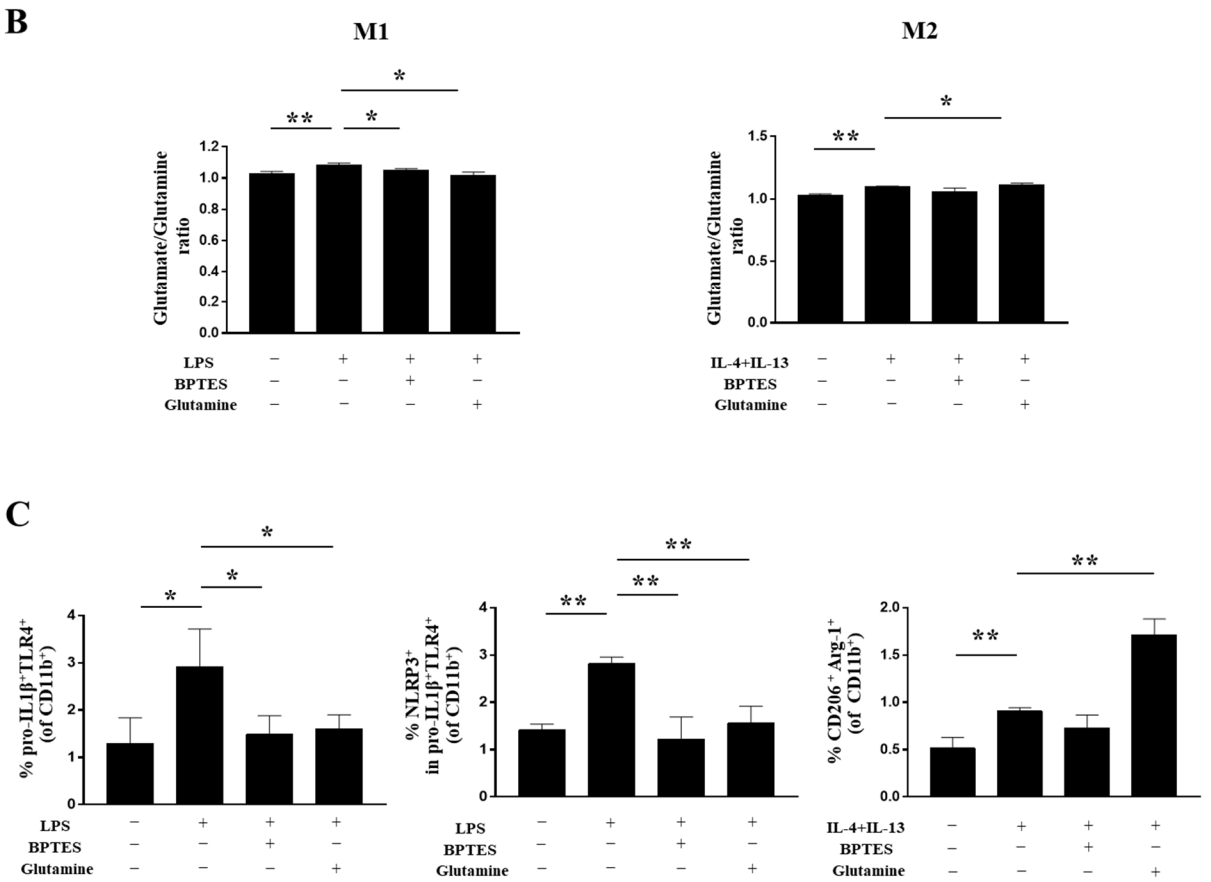

A, Representative gaiting strategy of TLR4^{+}Pro-IL-1β^{+} LPS-induced M1 macrophages, NLRP3^{+}TLR4^{+}Pro-IL1β^{+} LPS-induced M1 macrophages, and IL-4/IL-13-induced M2 macrophages (CD206^{+}Arg1^{+}) originating from an alveolar macrophage cell line. B, Glutamate to glutamine ratio in the cell lysate of each group. C, Frequencies of TLR4^{+}Pro-IL-1β^{+} cells, NLRP3^{+}TLR4^{+}Pro-IL-1β^{+} cells, and CD206^{+}Arg1^{+} cells in each group. *$p < 0.05$ and **$p < 0.01$. Statistical analysis determined by one-way ANOVA with Bonferroni's multiple comparisons test. LPS; lipopolysaccharide, BPTES; GLS1 inhibitor, TLR4; toll-like receptor 4, NLRP3; nucleotide-binding domain (NOD)-like receptor protein 3; Arg, arginine.

Figure 2-8. The effect of GLS1 inhibition and glutamine supplementation on the IL-17-producing ILC3s differentiated from ILCs in naïve mouse lungs in vitro

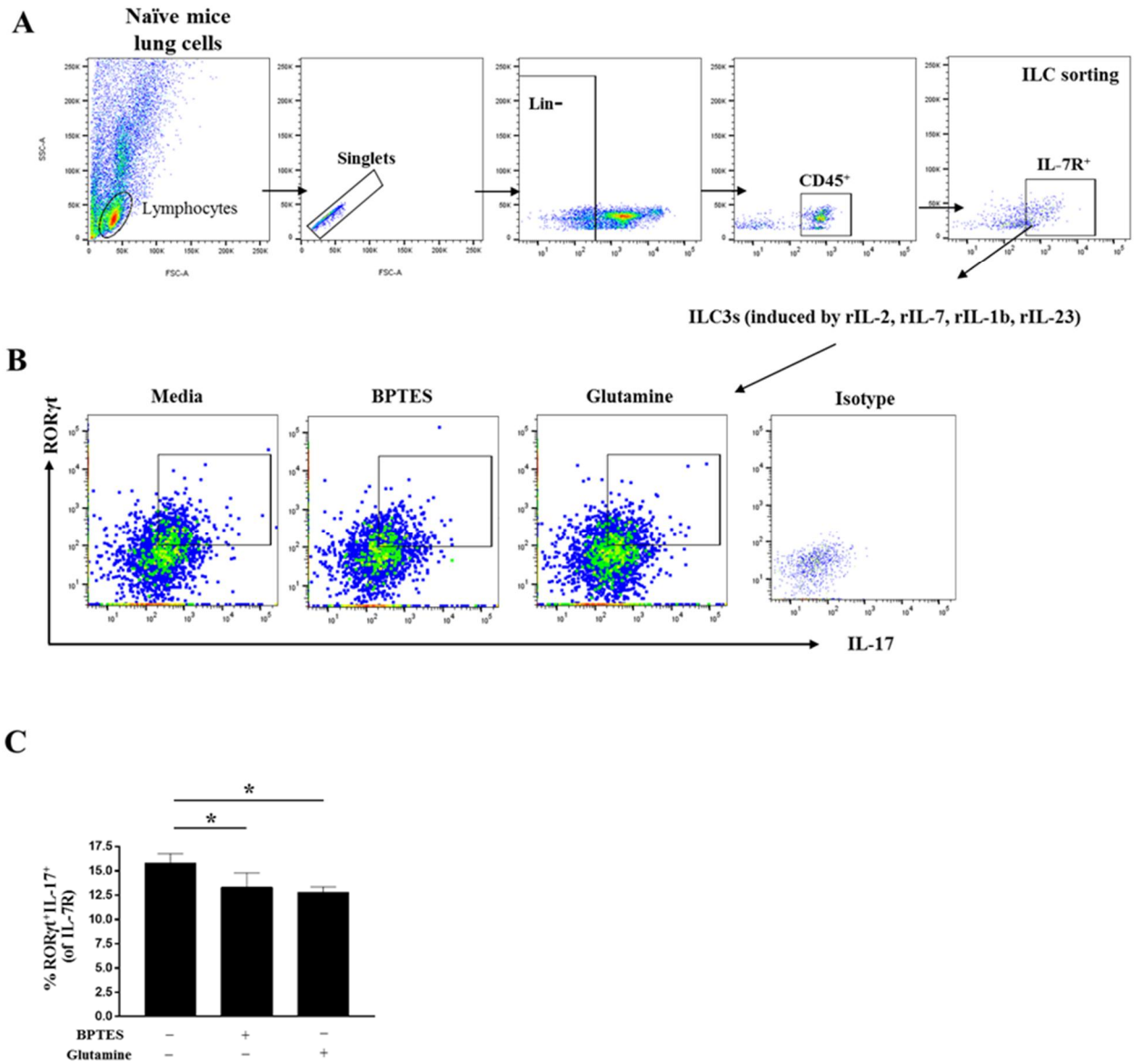

A, Representative gaiting strategy of RORγt^{+}IL-17^{+} ILC3s obtained from naïve mouse lung tissue. B-C, The gating plot and frequency of RORγt^{+}IL-17^{+} ILC3s in mouse lung tissue after culture. *$p < 0.05$. Statistical analysis determined by one-way ANOVA with Bonferroni's multiple comparisons test. ILC3; type 3 innate lymphoid cell, BPTES; GLS1 inhibitor

Figure 2-9. The levels of glutamine and glutamate in human plasma samples

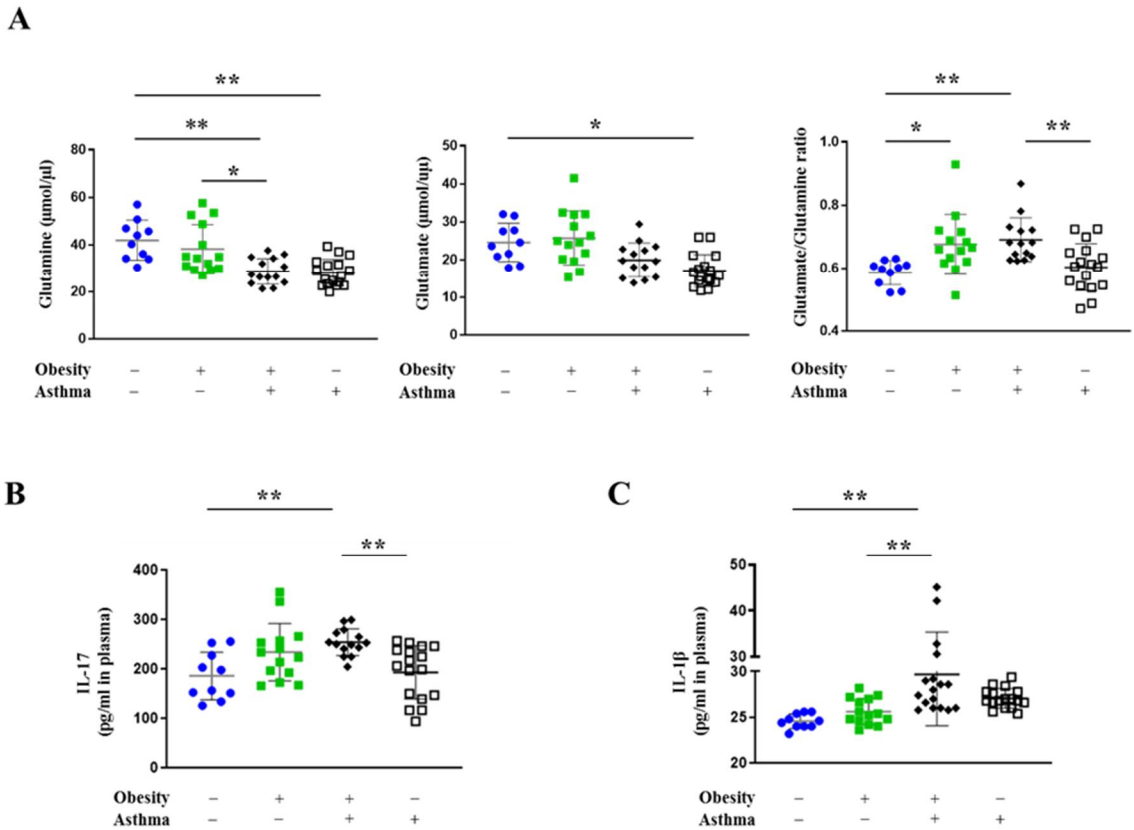

A, Levels of glutamine and glutamate, and glutamate to glutamine ratio. B, Levels of IL-17. C, Levels of IL-1β. *$p < 0.05$ and **$p < 0.01$.

Part II. Discussion

In this study, it was found that AHR in HFD-fed obese mice was prevented by inhibiting the conversion of glutamine to glutamate with BPTES, a GLS1 inhibitor. It was also observed that M1 macrophages increased, but M2 macrophages decreased in adipose tissue by HFD. BPTES did not affect the total numbers of M1 and M2 macrophages but decreased IL-1β^+ M1 macrophages, suggesting that this macrophage population is dependent on GLS1 activity. In addition, increased IL-1β^+ M1 macrophages in the lung tissue of HFD-fed obese mice were significantly attenuated after BPTES treatment. Similarly, ILC3s increased in the lung tissue of HFD-fed obese mice and were significantly decreased after BPTES treatment. These findings suggest that IL-1β^+ M1 macrophages and ILC3s are key immune cells in the pathogenesis of HFD-induced AHR and that this process may be reversed by inhibiting the first step of glutaminolysis, GLS1. In supporting these results obtained from in vivo and in vitro experiments, it was also observed that human plasma glutamate to glutamine ratios were significantly higher in obese asthmatics compared to non-obese asthmatics. The graphical abstract is presented in Fig. 2-10. To the best of my knowledge, this is the first study to investigate the pathophysiology of obese asthma, focusing on glutamine and its effects on immune cells, specifically macrophages and ILC3s.

It is well known that obese mice develop AHR, a major feature of asthma (88). IL-17 has been linked to AHR in obese mice, for instance, an HFD results in obesity but not AHR in IL-17 deficient mice (32), and increased lung IL-17 mRNA preceded

the development of AHR by several weeks in HFD-fed obese mice (89). However, in this study, there was no difference in lung Th17 cells after an HFD or an HFD plus BPTES treatment. Although a previous study revealed that diet-induced obesity promoted Th17 differentiation in adipose tissue (90), the results of this study suggested that lung Th17 cells are not affected by an HFD and ILC3s are the main source of IL-17 instead of Th17 cells. A previous report also showed that AHR in HFD-fed obese mice depended on innate immunity since AHR developed in obese $Rag^{-/-}$ mice (32). The onset of systemic inflammation coincided temporally with the development of AHR in HFD-fed obese mice, suggesting that possible interactions between systemic inflammation and IL-17 promote AHR (89). Likewise, current study observed that IL-1β^{+} M1 macrophages in lung tissue significantly increased. IL-1β activates the TLR4/NLRP3 signaling pathway and stimulates lung ILC3s to produce IL-17 and aggravate inflammation (32, 91).

This study observed that glutamine metabolism is a novel link between obesity and AHR in HFD-fed obese mice. Glutaminolysis, a major form of glutamine metabolism, consists of two steps. The first and most important step is the conversion of glutamine to glutamate by GLS1. The next step is the conversion of glutamate into α-KG by GDH. α-KG is converted to succinate and incorporated into the tricarboxylic acid cycle (92). Glutamine is not only an energy substrate but also a precursor of nucleic acids and nucleotide synthesis, and its metabolism is known to be involved in immunomodulation (93). Importantly, glutamine promotes M2 macrophage differentiation via the α-KG and glutamine-UDP-GlcNAc pathways (35).

Contrary to previous reports showing a reduction of adipose tissue glutamine levels in HFD-fed obese mice (35, 50, 93), this study observed that glutamine levels increased in serum, lung, and adipose tissue. The effect of an HFD on glutamine metabolism is varies depending on the cell type. For example, the long-term exposure of aged mice to an HFD led to increased glutamine levels in the liver and hippocampus via enhanced GS expression (94). Most of the previous studies evaluating the effect of glutamine metabolism on macrophages in adipose tissue have focused on GS (35, 50, 93, 94). However, GLS1 could be also important in the immunomodulation related with glutamine metabolism and the glutamate/glutamine ratio may be a good biomarker reflecting GLS1 activity. As shown in this study, an increase in the glutamate to glutamine ratio in the lung caused by an HFD favors M1 macrophage polarization rather than M2 macrophage polarization, leading to lung inflammation and can be reversed by treatment with BPTES. Moreover, in vitro experiments using BMDMs from naïve mice and a murine alveolar macrophage cell line showed that glutamine metabolism affected the TLR4/NLRP3 pathway, which is important for M1 macrophage activation. However, detailed mechanisms on how increased glutamate to glutamine ratio in HFD-fed obese mice is related to the TLR4/NLRP3 pathway and subsequent inflammation have been unknown so far.

This study found that GLS1 inhibitors reduced ILC3s in the lungs of HFD-induced obese mice. The number of IL-17-producing ILC3s differentiated from ILCs in the lungs of naïve mice decreased after BPTES or glutamine treatment, indicating that IL-17 production by ILC3s was also glutamine-dependent. In addition, this study observed that BPTES treatment attenuated HFD-induced peribronchial fibrosis. It was reported that peribronchial and perivascular fibrosis leads to AHR in HFD-

induced obese mice (95). Taken together, AHR in HFD-fed obese mice may be closely associated with augmented glutaminolysis.

According to previous studies, the glutamine level in human adipose tissue was lower in obese individuals than in non-obese individuals (48, 50). Serum from obese individuals displayed increased activity of GLS1 and decreased levels of GS, resulting in low serum glutamine and high glutamate levels (35, 50). Decreased levels of glutamate pyruvate transaminase, which converts glutamate to α-KG, also increased glutamate levels and decreased α-KG levels in obese individuals (96). Dysregulated glutamine metabolism was also investigated in several diseases, including Alzheimer's disease (AD), pulmonary fibrosis, psoriasis, and sepsis in obesity (97-100). In early AD mouse brain tissues, BPTES treatment reduced LPS-induced microglial activation and inflammation (98), and inhibition of GLS1 also attenuated collagen production and fibrosis in a pulmonary fibrosis mice model (97). In addition, glutamine administration decreased macrophage infiltration and inflammatory mediators such as IL-1β and IL-6 in an obese sepsis mouse model (100), and reduced both pro-inflammatory genes and macrophage infiltration in vivo in HFD mice adipose tissues and in vitro in human adipocytes (50). Human serum glutamate levels increased with an increase in visceral fat burden, and α-KG supplementation diminished the inflammation in adipose tissues and M1 macrophage polarization (35, 91, 96). Overall, each stage of glutamine metabolism is altered in obesity, and the changes in its metabolite levels promote inflammation and altered macrophage differentiation. Likewise, this study found that the plasma levels of glutamate, glutamine, IL-17, and IL-1β were higher in obese asthmatics than in non-obese asthmatics, suggesting a possible association between altered

glutamine metabolism and obesity-induced inflammation in humans. There have been two previous studies on the association between glutamine and asthma; however, they did not include obese asthmatics (101, 102). One study showed that glutamine supplementation resolved airway eosinophilia, mucus formation, AHR, and the production of Th2 cytokines by partly inhibiting the activity of cytosolic phospholipase A2 (102). In another study, it was reported that glutamine administration attenuated the allergic airway inflammation by upregulating MAPK phosphatase-1 expression in an OVA-challenged mouse model (101). Also, experimental glutamine-deficient OVA-challenged mice showed altered asthmatic features, such as neutrophilic airway inflammation but not eosinophilic inflammation (101). This study differs from the above studies in that HFD-induced obese mice represented a non-allergic asthma model, not a conventional allergic asthma model. This study suggests that the changes and impacts of glutaminolysis may differ depending on the type of effector cells involved in the pathophysiology of non-allergic asthma compared with allergic asthma.

This study has a few limitations. First, we examined only a small portion of the glutamine metabolism pathway. Further studies are required on glutamate and other glutamine metabolites, such as α-KG and succinate. Also, levels of GLS1 were not measured. Second, in human samples, we could only measure the levels of plasma metabolites and cytokines, and not the adipose tissue levels. The intake of dietary glutamine was not considered in the human samples. Next, this study did not exclude the possibility that the HFD-induced changes may be caused by differences in adiponectin and leptin, not altered glutamine metabolism. Finally, we only present descriptive findings that do not reveal the gene or transcriptional regulation of

glutamine metabolism. Additional experiments are needed to reveal the underlying mechanisms of these findings, especially the mechanism by which the inhibition of glutaminolysis reduces the activity of the LPS-TLR4-NLRP3-IL-1β and ILC3-RORγt-IL-17 pathways.

Figure 2-10. Graphical abstract

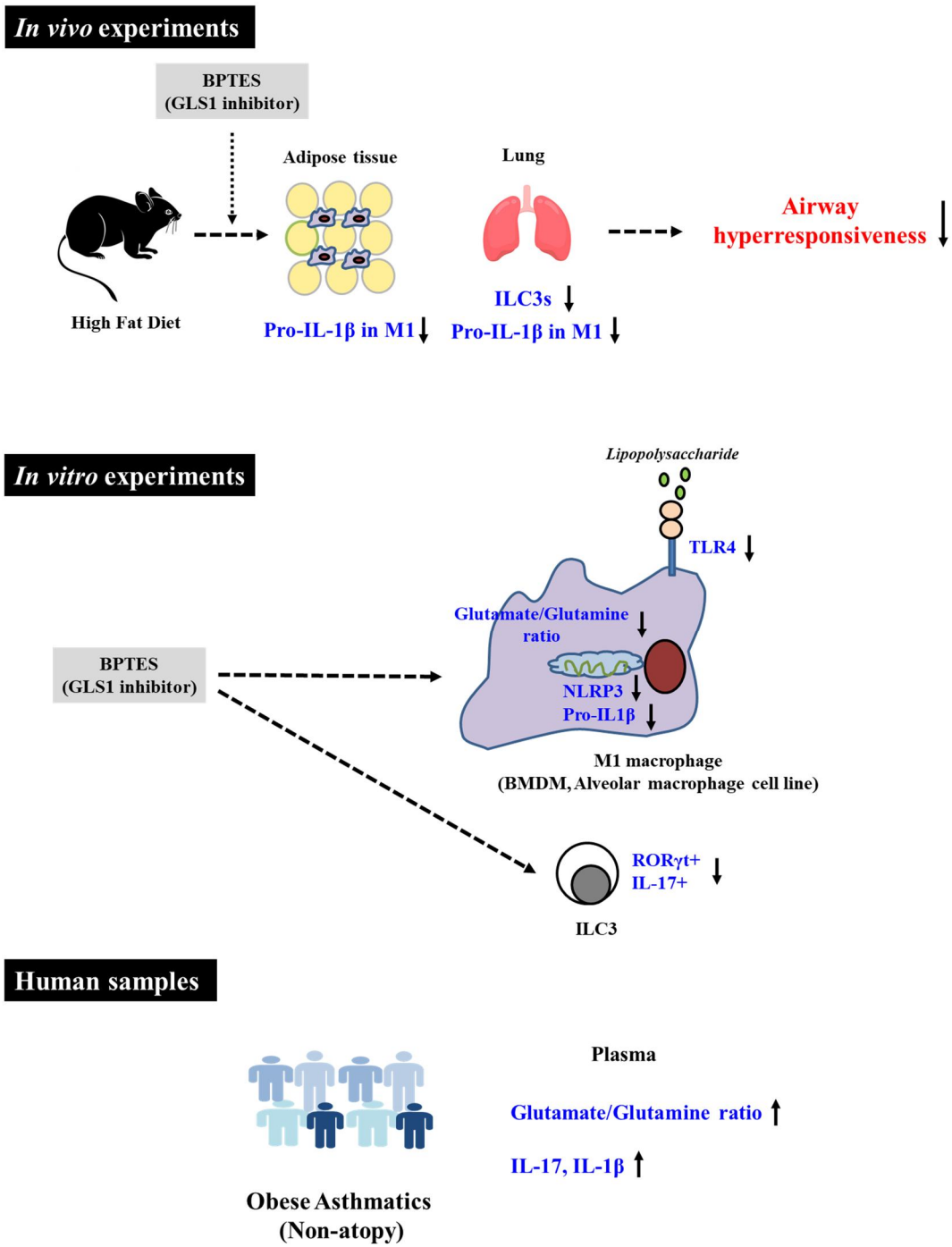

Conclusion

AHR, one of the important features of asthma, can be present in healthy people. This study showed that high BMI and FMI were associated with the development of AHR among healthy individuals. In addition, the group with newly developed AHR showed more loss of MM in the follow-up, suggesting that the distribution of FM and MM, and BMI, plays an important role in the development of AHR. A longitudinal study using a health checkup database confirmed that a gain of FM or a loss of MM over time is a risk factor for the development of AHR in otherwise healthy individuals. Sarcopenic obesity may increase the risk of AHR more than obesity alone in otherwise healthy individuals.

In the animal experiment for the mechanisms underlying obesity-related AHR, it was observed that altered glutamine metabolism played a role in the development of AHR induced by an HFD. The animal study also showed that IL-1β+NLRP3+ M1 macrophages and ILC3s are key immune cells in the pathogenesis of HFD-induced AHR, and was reversed by inhibiting the first step of glutaminolysis, GLS1, suggesting a link between altered glutamate to glutamine ratio and obesity-related asthma. A prospective study needs to be done to assess the role of FM reduction and dietary glutamine supplementation in preventing AHR development in obese healthy individuals.

References

1. Dixon AE, Peters U. The effect of obesity on lung function. Expert review of respiratory medicine. 2018;12(9):755-67.
2. Beuther DA, Sutherland ER. Overweight, obesity, and incident asthma: a meta-analysis of prospective epidemiologic studies. American journal of respiratory and critical care medicine. 2007;175(7):661-6.
3. Haldar P, Pavord ID, Shaw DE, Berry MA, Thomas M, Brightling CE, et al. Cluster analysis and clinical asthma phenotypes. American journal of respiratory and critical care medicine. 2008;178(3):218-24.
4. Dixon AE, Holguin F, Sood A, Salome CM, Pratley RE, Beuther DA, et al. An official American Thoracic Society Workshop report: obesity and asthma. Proceedings of the American Thoracic Society. 2010;7(5):325-35.
5. Brumpton BM, Camargo CA, Jr., Romundstad PR, Langhammer A, Chen Y, Mai XM. Metabolic syndrome and incidence of asthma in adults: the HUNT study. The European respiratory journal. 2013;42(6):1495-502.
6. Kim SH, Sutherland ER, Gelfand EW. Is there a link between obesity and asthma? Allergy, asthma & immunology research. 2014;6(3):189-95.
7. Assad N, Qualls C, Smith LJ, Arynchyn A, Thyagarajan B, Schuyler M, et al. Body mass index is a stronger predictor than the metabolic syndrome for future asthma in women. The longitudinal CARDIA study. American journal of respiratory and critical care medicine. 2013;188(3):319-26.
8. Holguin F, Bleecker ER, Busse WW, Calhoun WJ, Castro M, Erzurum SC, et al. Obesity and asthma: an association modified by age of asthma onset. The Journal of allergy and clinical immunology. 2011;127(6):1486-93.e2.
9. Chen Z, Salam MT, Alderete TL, Habre R, Bastain TM, Berhane K, et al. Effects of childhood asthma on the development of obesity among school-aged children. American journal of respiratory and critical care medicine. 2017;195(9):1181-8.
10. Mosen DM, Schatz M, Magid DJ, Camargo CA, Jr. The relationship between obesity and asthma severity and control in adults. The Journal of allergy

and clinical immunology. 2008;122(3):507-11.e6.
11. Jones RL, Nzekwu MM. The effects of body mass index on lung volumes. Chest. 2006;130(3):827-33.
12. Collet F, Mallart A, Bervar JF, Bautin N, Matran R, Pattou F, et al. Physiologic correlates of dyspnea in patients with morbid obesity. International journal of obesity (2005). 2007;31(4):700-6.
13. Juusela M, Poussa T, Kotaniemi J, Lundbäck B, Sovijärvi A. Bronchial hyperresponsiveness in a population of north Finland with no previous diagnosis of asthma or chronic bronchitis assessed with histamine and methacholine tests. International journal of circumpolar health. 2008;67(4):308-17.
14. Brutsche MH, Downs SH, Schindler C, Gerbase MW, Schwartz J, Frey M, et al. Bronchial hyperresponsiveness and the development of asthma and COPD in asymptomatic individuals: SAPALDIA cohort study. Thorax. 2006;61(8):671-7.
15. Shore SA. Obesity, airway hyperresponsiveness, and inflammation. Journal of applied physiology (Bethesda, Md : 1985). 2010;108(3):735-43.
16. Burgess JA, Matheson MC, Diao F, Johns DP, Erbas B, Lowe AJ, et al. Bronchial hyperresponsiveness and obesity in middle age: insights from an Australian cohort. The European respiratory journal. 2017;50(3).
17. Litonjua AA, Sparrow D, Celedon JC, DeMolles D, Weiss ST. Association of body mass index with the development of methacholine airway hyperresponsiveness in men: the Normative Aging Study. Thorax. 2002;57(7):581-5.
18. Schetz M, De Jong A, Deane AM, Druml W, Hemelaar P, Pelosi P, et al. Obesity in the critically ill: a narrative review. Intensive care medicine. 2019;45(6):757-69.
19. Hughes VA, Frontera WR, Roubenoff R, Evans WJ, Singh MA. Longitudinal changes in body composition in older men and women: role of body weight change and physical activity. The American journal of clinical nutrition. 2002;76(2):473-81.
20. Park HK, Lee SH, Lee SY, Kim SS, Park HW. Relationships between lung function decline and skeletal muscle and fat mass changes: a longitudinal study in healthy individuals. Journal of cachexia, sarcopenia and muscle. 2021;12(6):2145-

53.
21. Dietze J, Böcking C, Heverhagen JT, Voelker MN, Renz H. Obesity lowers the threshold of allergic sensitization and augments airway eosinophilia in a mouse model of asthma. Allergy. 2012;67(12):1519-29.
22. Calixto MC, Lintomen L, Schenka A, Saad MJ, Zanesco A, Antunes E. Obesity enhances eosinophilic inflammation in a murine model of allergic asthma. British journal of pharmacology. 2010;159(3):617-25.
23. Everaere L, Ait-Yahia S, Molendi-Coste O, Vorng H, Quemener S, LeVu P, et al. Innate lymphoid cells contribute to allergic airway disease exacerbation by obesity. The Journal of allergy and clinical immunology. 2016;138(5):1309-18.e11.
24. Shore SA, Schwartzman IN, Mellema MS, Flynt L, Imrich A, Johnston RA. Effect of leptin on allergic airway responses in mice. The Journal of allergy and clinical immunology. 2005;115(1):103-9.
25. Zheng H, Wu D, Wu X, Zhang X, Zhou Q, Luo Y, et al. Leptin promotes allergic airway inflammation through targeting the unfolded protein response pathway. Scientific reports. 2018;8(1):8905.
26. Miethe S, Karsonova A, Karaulov A, Renz H. Obesity and asthma. The Journal of allergy and clinical immunology. 2020;146(4):685-93.
27. Molofsky AB, Nussbaum JC, Liang HE, Van Dyken SJ, Cheng LE, Mohapatra A, et al. Innate lymphoid type 2 cells sustain visceral adipose tissue eosinophils and alternatively activated macrophages. The Journal of experimental medicine. 2013;210(3):535-49.
28. McLaughlin T, Liu LF, Lamendola C, Shen L, Morton J, Rivas H, et al. T-cell profile in adipose tissue is associated with insulin resistance and systemic inflammation in humans. Arteriosclerosis, thrombosis, and vascular biology. 2014;34(12):2637-43.
29. Lee MW, Odegaard JI, Mukundan L, Qiu Y, Molofsky AB, Nussbaum JC, et al. Activated type 2 innate lymphoid cells regulate beige fat biogenesis. Cell. 2015;160(1-2):74-87.
30. Bhatraju NK, Agrawal A. Mitochondrial dysfunction linking obesity and asthma. Annals of the American Thoracic Society. 2017;14(Supplement_5):S368-s73.

31. Nguyen DV, Linderholm A, Haczku A, Kenyon N. Obesity-related, metabolic asthma: a new role for glucagon-like peptide 1 agonists. The Lancet Respiratory medicine. 2017;5(3):162-4.
32. Kim HY, Lee HJ, Chang YJ, Pichavant M, Shore SA, Fitzgerald KA, et al. Interleukin-17-producing innate lymphoid cells and the NLRP3 inflammasome facilitate obesity-associated airway hyperreactivity. Nature medicine. 2014;20(1):54-61.
33. Sharma N, Akkoyunlu M, Rabin RL. Macrophages-common culprit in obesity and asthma. Allergy. 2018;73(6):1196-205.
34. Bantulà M, Roca-Ferrer J, Arismendi E, Picado C. Asthma and obesity: two diseases on the rise and bridged by inflammation. Journal of clinical medicine. 2021;10(2).
35. Ren W, Xia Y, Chen S, Wu G, Bazer FW, Zhou B, et al. Glutamine metabolism in macrophages: a novel target for obesity/type 2 diabetes. Advances in nutrition (Bethesda, Md). 2019;10(2):321-30.
36. Shapouri-Moghaddam A, Mohammadian S, Vazini H, Taghadosi M, Esmaeili SA, Mardani F, et al. Macrophage plasticity, polarization, and function in health and disease. Journal of cellular physiology. 2018;233(9):6425-40.
37. Olefsky JM, Glass CK. Macrophages, inflammation, and insulin resistance. Annual review of physiology. 2010;72:219-46.
38. Yuan Y, Ran N, Xiong L, Wang G, Guan X, Wang Z, et al. Obesity-related asthma: immune regulation and potential targeted therapies. Journal of immunology research. 2018;2018:1943497.
39. Liang L, Hur J, Kang JY, Rhee CK, Kim YK, Lee SY. Effect of the anti-IL-17 antibody on allergic inflammation in an obesity-related asthma model. The Korean journal of internal medicine. 2018;33(6):1210-23.
40. Agache I, Ciobanu C, Agache C, Anghel M. Increased serum IL-17 is an independent risk factor for severe asthma. Respiratory medicine. 2010;104(8):1131-7.
41. Sasaki T, Moro K, Kubota T, Kubota N, Kato T, Ohno H, et al. Innate lymphoid cells in the induction of obesity. Cell reports. 2019;28(1):202-17.e7.
42. Artis D, Spits H. The biology of innate lymphoid cells. Nature.

2015;517(7534):293-301.
43. Williams EJ, Negewo NA, Baines KJ. Role of the NLRP3 inflammasome in asthma: Relationship with neutrophilic inflammation, obesity, and therapeutic options. The Journal of allergy and clinical immunology. 2021;147(6):2060-2.
44. Lee YS, Wollam J, Olefsky JM. An integrated view of immunometabolism. Cell. 2018;172(1-2):22-40.
45. Ardawi MS, Newsholme EA. Maximum activities of some enzymes of glycolysis, the tricarboxylic acid cycle and ketone-body and glutamine utilization pathways in lymphocytes of the rat. The Biochemical journal. 1982;208(3):743-8.
46. Newsholme P, Curi R, Gordon S, Newsholme EA. Metabolism of glucose, glutamine, long-chain fatty acids and ketone bodies by murine macrophages. The Biochemical journal. 1986;239(1):121-5.
47. Lecoutre S, Maqdasy S, Petrus P, Ludzki A, Couchet M, Mejhert N, et al. Glutamine metabolism in adipocytes: a bona fide epigenetic modulator of inflammation. Adipocyte. 2020;9(1):620-5.
48. Wahl S, Yu Z, Kleber M, Singmann P, Holzapfel C, He Y, et al. Childhood obesity is associated with changes in the serum metabolite profile. Obesity facts. 2012;5(5):660-70.
49. Bagheri M, Farzadfar F, Qi L, Yekaninejad MS, Chamari M, Zeleznik OA, et al. Obesity-related metabolomic profiles and discrimination of metabolically unhealthy obesity. Journal of proteome research. 2018;17(4):1452-62.
50. Petrus P, Lecoutre S, Dollet L, Wiel C, Sulen A, Gao H, et al. Glutamine links obesity to inflammation in human white adipose tissue. Cell metabolism. 2020;31(2):375-90.e11.
51. Martin-Sanchez FJ, Aguiar-Pulido V, Lopez-Campos GH, Peek N, Sacchi L. Secondary use and analysis of big data collected for patient care. Yearbook of medical informatics. 2017;26(1):28-37.
52. Jansen DF, Schouten JP, Vonk JM, Rijcken B, Timens W, Kraan J, et al. Smoking and airway hyperresponsiveness especially in the presence of blood eosinophilia increase the risk to develop respiratory symptoms: a 25-year follow-up study in the general adult population. American journal of respiratory and critical care medicine. 1999;160(1):259-64.

53. Pellegrino R, Viegi G, Brusasco V, Crapo RO, Burgos F, Casaburi R, et al. Interpretative strategies for lung function tests. The European respiratory journal. 2005;26(5):948-68.
54. Choi JK, Paek D, Lee JO. Normal predictive values of spirometry in Korean population. The Korean Academy of Tuberculosis and Respiratory Diseases. 2005;58(3):230-42.
55. Crapo RO, Casaburi R, Coates AL, Enright PL, Hankinson JL, Irvin CG, et al. Guidelines for methacholine and exercise challenge testing-1999. This official statement of the American Thoracic Society was adopted by the ATS Board of Directors, July 1999. American journal of respiratory and critical care medicine. 2000;161(1):309-29.
56. Janssen I, Heymsfield SB, Baumgartner RN, Ross R. Estimation of skeletal muscle mass by bioelectrical impedance analysis. Journal of applied physiology (Bethesda, Md : 1985). 2000;89(2):465-71.
57. Kyle UG, Genton L, Hans D, Pichard C. Validation of a bioelectrical impedance analysis equation to predict appendicular skeletal muscle mass (ASMM). Clinical nutrition (Edinburgh, Scotland). 2003;22(6):537-43.
58. van Veen IH, Ten Brinke A, Sterk PJ, Rabe KF, Bel EH. Airway inflammation in obese and nonobese patients with difficult-to-treat asthma. Allergy. 2008;63(5):570-4.
59. Livnat G, Yoseph RB, Nir V, Hakim F, Yigla M, Bentur L. Evaluation of high-sensitivity serum CRP levels compared to markers of airway inflammation and allergy as predictors of methacholine bronchial hyper-responsiveness in children. Lung. 2015;193(1):39-45.
60. Shimoda T, Obase Y, Kishikawa R, Iwanaga T. Serum high-sensitivity C-reactive protein can be an airway inflammation predictor in bronchial asthma. Allergy and asthma proceedings. 2015;36(2):e23-8.
61. Ponti F, Santoro A, Mercatelli D, Gasperini C, Conte M, Martucci M, et al. Aging and imaging assessment of body composition: from fat to facts. Frontiers in endocrinology. 2019;10:861.
62. Bone AE, Hepgul N, Kon S, Maddocks M. Sarcopenia and frailty in chronic respiratory disease. Chronic respiratory disease. 2017;14(1):85-99.

63. Baracos VE, Arribas L. Sarcopenic obesity: hidden muscle wasting and its impact for survival and complications of cancer therapy. Annals of oncology : official journal of the European Society for Medical Oncology. 2018;29(suppl_2):ii1-ii9.
64. Koo HK, Park JH, Park HK, Jung H, Lee SS. Conflicting role of sarcopenia and obesity in male patients with chronic obstructive pulmonary disease: Korean National Health and Nutrition Examination Survey. PloS one. 2014;9(10):e110448.
65. Wannamethee SG, Atkins JL. Muscle loss and obesity: the health implications of sarcopenia and sarcopenic obesity. The Proceedings of the Nutrition Society. 2015;74(4):405-12.
66. Salome CM, Munoz PA, Berend N, Thorpe CW, Schachter LM, King GG. Effect of obesity on breathlessness and airway responsiveness to methacholine in non-asthmatic subjects. International journal of obesity (2005). 2008;32(3):502-9.
67. Sampson MG, Grassino AE. Load compensation in obese patients during quiet tidal breathing. Journal of applied physiology: respiratory, environmental and exercise physiology. 1983;55(4):1269-76.
68. Boulet LP, Turcotte H, Martin J, Poirier P. Effect of bariatric surgery on airway response and lung function in obese subjects with asthma. Respiratory medicine. 2012;106(5):651-60.
69. Hohlfeld JM, Schmiedl A, Erpenbeck VJ, Venge P, Krug N. Eosinophil cationic protein alters pulmonary surfactant structure and function in asthma. The Journal of allergy and clinical immunology. 2004;113(3):496-502.
70. Chung KF, Barnes PJ. Cytokines in asthma. Thorax. 1999;54(9):825-57.
71. Soutar A, Seaton A, Brown K. Bronchial reactivity and dietary antioxidants. Thorax. 1997;52(2):166-70.
72. Weiss ST. Obesity: insight into the origins of asthma. Nature immunology. 2005;6(6):537-9.
73. Kim JM, Im YN, Chung YJ, Youm JH, Im SY, Han MK, et al. Glutamine deficiency shifts the asthmatic state toward neutrophilic airway inflammation. Allergy. 2022;77(4):1180-91.
74. Dutta P, Le A, Vander Jagt DL, Tsukamoto T, Martinez GV, Dang CV, et

al. Evaluation of LDH-A and glutaminase inhibition in vivo by hyperpolarized 13C-pyruvate magnetic resonance spectroscopy of tumors. Cancer research. 2013;73(14):4190-5.
75. Xiang Y, Stine ZE, Xia J, Lu Y, O'Connor RS, Altman BJ, et al. Targeted inhibition of tumor-specific glutaminase diminishes cell-autonomous tumorigenesis. The Journal of clinical investigation. 2015;125(6):2293-306.
76. Shalaby KH, Gold LG, Schuessler TF, Martin JG, Robichaud A. Combined forced oscillation and forced expiration measurements in mice for the assessment of airway hyperresponsiveness. Respiratory research. 2010;11(1):82.
77. Shim JS, Lee HS, Park DE, Won Lee J, Bae B, Chang Y, et al. Aggravation of asthmatic inflammation by chlorine exposure via innate lymphoid cells and CD11c(intermediate) macrophages. Allergy. 2020;75(2):381-91.
78. Zhang L, Mosoian A, Schwartz ME, Florman SS, Gunasekaran G, Schiano T, et al. HIV infection modulates IL-1β response to LPS stimulation through a TLR4-NLRP3 pathway in human liver macrophages. Journal of leukocyte biology. 2019;105(4):783-95.
79. Besnard AG, Guillou N, Tschopp J, Erard F, Couillin I, Iwakura Y, et al. NLRP3 inflammasome is required in murine asthma in the absence of aluminum adjuvant. Allergy. 2011;66(8):1047-57.
80. Ying W, Cheruku PS, Bazer FW, Safe SH, Zhou B. Investigation of macrophage polarization using bone marrow derived macrophages. Journal of visualized experiments : JoVE. 2013(76).
81. Liang M, Wang X, Yuan Y, Zhou Q, Tong C, Jiang W. Different effect of glutamine on macrophage tumor necrosis factor-alpha release and heat shock protein 72 expression in vitro and in vivo. Acta biochimica et biophysica Sinica. 2009;41(2):171-7.
82. Ajaz S, McPhail MJ, Singh KK, Mujib S, Trovato FM, Napoli S, et al. Mitochondrial metabolic manipulation by SARS-CoV-2 in peripheral blood mononuclear cells of patients with COVID-19. American journal of physiology Cell physiology. 2021;320(1):C57-c65.
83. Yang D, Guo X, Huang T, Liu C. The role of group 3 innate lymphoid cells in lung infection and immunity. Frontiers in cellular and infection

microbiology. 2021;11:586471.
84. Lim JU, Lee JH, Kim JS, Hwang YI, Kim TH, Lim SY, et al. Comparison of World Health Organization and Asia-Pacific body mass index classifications in COPD patients. International journal of chronic obstructive pulmonary disease. 2017;12:2465-75.
85. Duan M, Steinfort DP, Smallwood D, Hew M, Chen W, Ernst M, et al. CD11b immunophenotyping identifies inflammatory profiles in the mouse and human lungs. Mucosal immunology. 2016;9(2):550-63.
86. Poole JA, Gleason AM, Bauer C, West WW, Alexis N, van Rooijen N, et al. CD11c(+)/CD11b(+) cells are critical for organic dust-elicited murine lung inflammation. American journal of respiratory cell and molecular biology. 2012;47(5):652-9.
87. Celik M, Labuz D, Keye J, Glauben R, Machelska H. IL-4 induces M2 macrophages to produce sustained analgesia via opioids. JCI insight. 2020;5(4).
88. Zhu M, Williams AS, Chen L, Wurmbrand AP, Williams ES, Shore SA. Role of TNFR1 in the innate airway hyperresponsiveness of obese mice. Journal of applied physiology (Bethesda, Md : 1985). 2012;113(9):1476-85.
89. Mathews JA, Wurmbrand AP, Ribeiro L, Neto FL, Shore SA. Induction of IL-17A precedes development of airway hyperresponsiveness during diet-induced obesity and correlates with complement factor D. Frontiers in immunology. 2014;5:440.
90. Endo Y, Yokote K, Nakayama T. The obesity-related pathology and Th17 cells. Cellular and molecular life sciences : CMLS. 2017;74(7):1231-45.
91. Leiria LO, Martins MA, Saad MJ. Obesity and asthma: beyond T(H)2 inflammation. Metabolism: clinical and experimental. 2015;64(2):172-81.
92. Halama A, Suhre K. Advancing cancer treatment by targeting glutamine metabolism-a roadmap. Cancers. 2022;14(3).
93. Miyajima M. Amino acids: key sources for immunometabolites and immunotransmitters. International immunology. 2020;32(7):435-46.
94. Soontornniyomkij V, Kesby JP, Soontornniyomkij B, Kim JJ, Kisseleva T, Achim CL, et al. Age and high-fat diet effects on glutamine synthetase immunoreactivity in liver and hippocampus and recognition memory in mice.

Current aging science. 2016;9(4):301-9.
95. Park YH, Oh EY, Han H, Yang M, Park HJ, Park KH, et al. Insulin resistance mediates high-fat diet-induced pulmonary fibrosis and airway hyperresponsiveness through the TGF-β1 pathway. Experimental & molecular medicine. 2019;51(5):1-12.
96. Maltais-Payette I, Boulet MM, Prehn C, Adamski J, Tchernof A. Circulating glutamate concentration as a biomarker of visceral obesity and associated metabolic alterations. Nutrition & metabolism. 2018;15:78.
97. Cui H, Xie N, Jiang D, Banerjee S, Ge J, Sanders YY, et al. Inhibition of glutaminase 1 attenuates experimental pulmonary fibrosis. American journal of respiratory cell and molecular biology. 2019;61(4):492-500.
98. Gao G, Zhao S, Xia X, Li C, Li C, Ji C, et al. Glutaminase C regulates microglial activation and pro-inflammatory exosome release: relevance to the pathogenesis of Alzheimer's disease. Frontiers in cellular neuroscience. 2019;13:264.
99. Xia X, Cao G, Sun G, Zhu L, Tian Y, Song Y, et al. GLS1-mediated glutaminolysis unbridled by MALT1 protease promotes psoriasis pathogenesis. The Journal of clinical investigation. 2020;130(10):5180-96.
100. Yeh CL, Su LH, Wu JM, Yang PJ, Lee PC, Chen PD, et al. Effects of the glutamine administration on T helper cell regulation and inflammatory response in obese mice complicated with polymicrobial sepsis. Mediators Inflamm. 2020;2020:8869017.
101. Kim JM, Im YN, Chung YJ, Youm JH, Im SY, Han MK, et al. Glutamine deficiency shifts the asthmatic state toward neutrophilic airway inflammation. Allergy. 2021.
102. Ko HM, Kang NI, Kim YS, Lee YM, Jin ZW, Jung YJ, et al. Glutamine preferentially inhibits T-helper type 2 cell-mediated airway inflammation and late airway hyperresponsiveness through the inhibition of cytosolic phospholipase A(2) activity in a murine asthma model. Clinical and experimental allergy : journal of the British Society for Allergy and Clinical Immunology. 2008;38(2):357-64.

국문 초록

고지방식이 마우스의 기도과민성 발생에서 글루타민분해효소의 역할

심지수

서울대학교 대학원

의학과 내과학 전공

서론: 기도과민성은 만성 염증성 기도질환인 천식의 주된 특징 중 하나로, 비만과도 연관되어 있는 것으로 알려져 있다. 비만은 일반적으로 체중과 신장을 바탕으로 한 체질량지수를 통해 정의된다. 그러나 체중은 체지방량과 근육량 두 가지로 구성되며, 이러한 체지방량과 근육량의 조성은 시간에 따라 변화한다. 따라서 체질량지수 뿐만 아니라 체지방량 및 근육량의 변화와 기도과민성 간의 연관성을 확인할 수 있는 종단 연구가 필요하다. 또한 최근에는 체내 대사와 면역계 사이의 밀접한 연관성이 제시되면서, 특히 비만에서는 글루타민의 대사 이상이 여러 면역세포의 변화를 초래하여 염증을 증가시킨다는 보고들이 있었다. 이러한 글루타민 대사 이상이 비만과 기도과민성 간의 연관성을 설명할 수 있는 기전 중 하나일 가능성이 있다. 그러나 현재까지 이에 대한 연구는 부족한 실정이다.

방법: 서울대학교병원 강남센터의 건강검진 자료를 이용하여 비만과 기도과민성 유도 사이의 연관성을 규명하는 횡단 및 종단 연구를 수행하였다. 메타콜린 기관지 유발시험을 최소 3년 간격으로 2차례 시행한 정상인 검진 수진자를 모집하였고, 대상자들은 매 건강검진시마다 생체전기저항분석을 통하여 체지방지수와 근육량지수를 확인하였다. 추적관찰에서 기도과민성이 새롭게 발생한 대상자와 그렇지 않은 대상자 간의 체지방지수 및 근육량지수의 변화가 있는지 분석하였다. 또한 비만으로 인한 기도과민성 발생에 있어 글루타민 대사 이상의 역할을 확인하기 위하여 마우스 실험을 수행하였다. 4주령의 C57BL/6 마우스를 대상으로 13주간 고지방 식이를 시행하였고, 이를 글루타민 분해효소를 억제하는 BPTES (Bis-2-[5-phenylacetamido-1,3,4-thiadiazol-2-yl]ethyl sulfide)를 처리한 군과 처리하지 않은 군으로 나누어 마우스의 기도과민성을 측정하고 혈액, 폐와 지방조직을 얻어 분석하였다. 추가적으로 마우스 골수유래 대식세포와 폐포대식세포주를 이용한 생체 외 실험을 시행하였고, 마지막으로 정상 체중 천식 환자와 비만 천식 환자의 혈액을 수집하여 혈장 내 글루타민과 글루탐산 수치를 측정하였다.

결과: 건강검진 수진자를 대상으로 한 횡단연구에는 총 4,023명 (여성 1,290명, 남성 2,733명)이 등록되었고, 그 중 첫 건강검진에서 이미 기도과민성을 보인 대상자가 112명이었다. 다변량 분석에서 체지방지수가 높을수록 기도과민성을 보유하고 있을 위험도가 유의하게 높았고 (오즈비 = 1.37, 95% 신뢰구간: 1.06-1.76, p = 0.017), 기도과민성을 보인

112명의 수진자를 대상으로 한 상관관계 분석에서는 체지방지수와 1초간 노력성 호기량이 20% 감소될 때의 메타콜린 농도 (PC20)가 유의한 음의 상관관계를 보였다 (R = −0.31, p = 0.00087). 종단연구에는 총 283명 (여성 61명, 남성 267명)이 등록되었다. 생체전기저항분석 측정 평균 횟수는 6.96회 (사분위수 범위: 5−9), 평균 추적기간은 6.69년 (사분위수 범위: 4.63−8.36)이었다. 총 13명의 대상자가 추적관찰에서 기도과민성이 발생하였고, 기도과민성 발생군과 비발생군 간의 기저 특성은 흡연 외에는 유의한 차이가 없었다. 추적기간 중, 모든 대상자들은 체지방량이 증가하고 근육량이 감소하였는데 기도과민성 발생군에서 비발생군에 비해 체지방량이 좀 더 증가하는 경향을 보였다 (p = 0.057). 또한 기도과민성 발생군에서 비 발생군에 비해 근육량지수가 더 유의하게 감소하였다 (p = 0.011). 다변량 분석에서는 체지방지수 변화율 ([kg/m^2]/year)이 기도과민성 발생의 위험도와 유의한 상관관계를 보였다 (오즈비 = 1.114x10^4, 95% 신뢰구간: 1.192-1.551x10^8, p = 0.037). 고지방식이 마우스 실험에서는 알레르겐 감작 없이도 고지방식이로 인하여 기도과민성이 유도됨을 확인하였다. BPTES 처리를 했을 때 이러한 기도과민성이 유의하게 감소하였고, 폐조직의 IL−1β^+ M1 대식세포와 제3형 선천성 림프구 세포 역시 유의하게 감소하였다. 골수유래 대식세포와 폐포대식세포주를 이용한 생체 외 실험에서는 lipopolysaccharide에 의해 유도된 IL−1β^+NLRP3$^+$ M1 대식세포의 비율이 BPTES 처리와 글루타민 공급에 의해 유의하게 감소함을 확인하

였다. 또한 나이브 마우스의 폐조직에서 BPTES 처리는 IL-17을 생성하는 제3형 선천성 림프구 세포의 감소를 유도하였다. 끝으로 비만한 천식 환자에서 정상 체중 천식 환자에 비해 혈청 글루탐산/글루타민 비율이 유의하게 증가되어 있음을 확인하였다.

결론: 건강검진 수진자료를 이용한 횡단 및 종단연구를 통해 정상인에서 시간에 따른 체지방량의 증가와 근육량의 감소가 기도과민성 발생의 위험인자임을 밝혔다. 비만이 기도과민성을 유도하는 기전을 밝히기 위해 시행한 마우스 연구에서는 고지방식이에 의한 기도과민성의 발생에 있어 글루타민 대사 이상이 관여함을 밝혔다. 특히 고지방식이에 의한 기도과민성에는 IL-1β^{+}NLRP3^{+} M1 대식세포와 제3형 선천성 림프구 세포가 핵심적으로 관여하는 면역세포이며, 글루타민 분해경로의 첫번째 단계의 효소를 억제함으로써 이러한 면역세포와 기도과민성이 감소함을 보였다. 본 연구 내용을 바탕으로 향후 정상인의 기도과민성 발생 예방에 있어 체지방량 감소와 글루타민 공급의 역할에 대한 추가적인 전향적 연구가 필요할 것으로 생각된다.

주요어:
천식; 기도과민성; 체지방량; 비만; 글루타민; 고지방식이 마우스; 선천성 림프구 세포; 대식세포.

학번: 2017-33616